AEROSOLITUTKIMUSSEURA R.Y.
FINNISH ASSOCIATION FOR AEROSOL RESEARCH
REPORT SERIES IN AEROSOL SCIENCE
№ 176

Kimmo Neitola

Experimental studies on nucleation and new particle formation

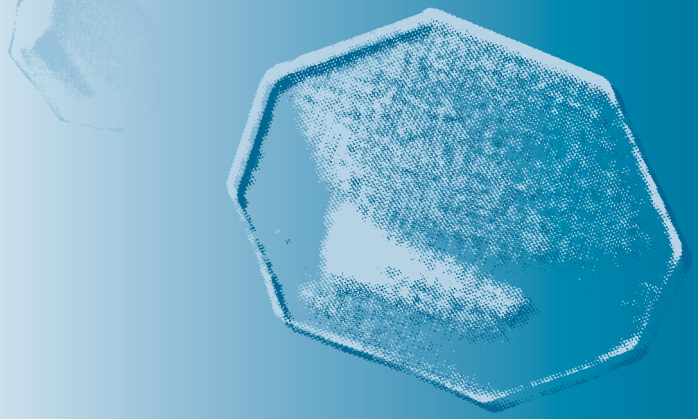

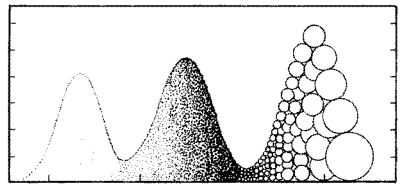

REPORT SERIES IN AEROSOL SCIENCE Kimmo Neitola

№ 176 2015

Report Series in Aerosol Science

166. Ditte Mogensen, "Insights into atmospheric oxidation" (2015)
167. Silja Häme (née Häkkinen), "Nanoparticle volatility and growth: Implications for interactions between biogenic and anthropogenic aerosol components" (2015)
168. Jouni Heiskanen, "Lake-atmosphere greenhouse gas exchange in relation to atmospheric forcing and lake bio-geochemistry" (2015)
169. Mikhail Paramonov, "Life cycle of a cloud condensation nucleus, CCN" (2015)
170. Johanna Patokoski, "Influence of source types and source areas on the concentrations of volatile organic compounds in Southern Finland" (2015)
171. Maija Kajos, "Emissions, concentrations and effects of BVOCs in the boreal atmosphere" (2015)
172. Tuija Jokinen, "Formation of low-volatility aerosol precursor molecules and clusters in the atmosphere" (2015)
173. Juha Kangasluoma, "Generation, characterization and sizing of sub-3 nm nanoparticles and molecular clusters" (2015)
174. Luxi Zhou, "Modelling aerosol formation and precursor gases in the boundary layer" (2015)
175. Jarno Ruusunen, "Studies of nanoparticle synthesis and physicochemical properties of aerosols" (2015)
176. Kimmo Neitola, "Experimental studies on nucleation and new particle formation" (2015)

Aerosolitutkimusseura ry
Helsinki 2015
ISSN 0784-3496
ISBN 978-952-7091-38-8

REPORT SERIES IN AEROSOL SCIENCE
N:o 176 (2015)

EXPERIMENTAL STUDIES ON NUCLEATION AND NEW PARTICLE FORMATION

KIMMO NEITOLA

Finnish Meteorological Institute
Helsinki, Finland

Division of Atmospheric Sciences
Department of Physics
Faculty of Science
University of Helsinki
Helsinki, Finland

Academic dissertation

To be presented, with the permission of the Faculty of Science of the University of Helsinki, for public criticism in auditorium Brainstorm, Erik Palménin aukio 1, on October 30th, 2015, at 12 o'clock noon.

Helsinki 2015

Author's Address: Finnish Meteorological Institute
P.O. Box 503
FI-00101, Helsinki, Finland
kimmo.neitola@fmi.fi

Supervisors: Professor Markku Kulmala, Ph.D.
Department of Physics
University of Helsinki

David Brus, Ph.D.
Atmospheric Composition Research
Finnish Meteorological Institute

Docent, Heikki Lihavainen, Ph.D.
Atmospheric Composition Research
Finnish Meteorological Institute

Reviewers: Professor Annele Virtanen, Ph.D.
Department of Applied Physics
University of Eastern Finland

Professor Joachim Curtius, Ph.D.
Department of Geosciences
Goethe University, Frankfurt

Opponent: Professor James Smith, Ph.D.
Department of Chemistry
University of California, Irvine

ISBN 978-952-7091-38-8 (printed version)
ISSN 0784-3496
Helsinki 2015
Unigrafia Oy

ISBN 978-952-7091-39-5 (pdf version)
http://ethesis.helsinki.fi
Helsinki 2015
Helsingin yliopiston verkkojulkaisut

Acknowledgements

The work for this thesis was done in the Atmospheric Aerosols group in the Finnish Meteorological Institute. I am grateful for the head of Research and Development division Prof. Yrjö Viisanen for providing me the working facilities. I would like to thank Doc. Heikki Lihavainen for hiring me in to his group and Dr. Eija Asmi for keeping me on the payroll.

I would like to thank Prof. Markku Kulmala for supervision and encouragement towards such an interesting field of science.

I thank Prof. Annele Virtanen and Prof. Joachim Curtius for reviewing this thesis.

I thank Prof. Tuukka Petäjä for the great help with my thesis.

Since I started working with science, I have met wonderful people not only to work with, but also to play with. Whether it has been work trips around the globe or just few beers near Kumpula, you people have kept me sane and made me laugh. I would like to show my appreciation to you all. Special thanks goes to Eija for being my roommate and tolerating my complaints on the southern side of the planet. Also, special thanks for Mikko, who was the first person I met when I started my work within science. You are a great traveling companion and you know when a man needs a beer.

I would like to thank all the group members at Finnish Meteorological Institute, especially my supervisor and a great friend David Brus. You have thought me a lot, not only about science and measurements, but also about life. Thank you for all the long hours in the lab and even longer in the sauna at Pallasjärvi. I am truly grateful for your help and support. Also great thanks to Antti for the numerous conference and Pallas trips, it's good to have a friend, who understands that life is just a part of football!

I would like to thank all my great friends for alienating me from my work from time to time and making it possible to enjoy life. Whether it has been fishing in Lapland with Roope or debate about science in the long hours of night with Atte, you guys made it easy to forget work for a while. Special thanks to my old friend Gissa, without your competition, I wouldn't have had the interest to continue this far.

I would like to show appreciation to my physics teacher, late Osmo Rautava, who inspired me towards science much more than anyone else.

Great thanks goes to my mom and dad, who supported me in my studies and had always place to come, even though I moved to the opposite side of the country. I couldn't have done this without you.

Finally, my greatest appreciation goes to my wife Hanna. You supported me on the rough spots and laughed with me when it was time for it. You managed through all my work trips and stayed even when I missed our honeymoon. You are my inspiration to life, Giitu!

Experimental studies on nucleation and new particle formation.

Kimmo Antero Neitola

University of Helsinki, 2015

Abstract

Aerosols affect our everyday life in many ways. Changes in visibility, allergies to pollen, spray cans and dosing of some medication are just a few examples of common aerosols. Aerosols may have more profound way to affect every one of us; through climate. Possible changes in aerosol particle concentrations and compositions may alter large precipitation patterns and change cloud albedo, and lifetime. To be able to predict future changes in climate, profound understating of physical and chemical processes affecting the atmospheric aerosol population is crucial.

Nucleation, i.e. gas-to-liquid phase transition, is the fundamental step in particle formation in the atmosphere. Sulphuric acid is established to be one of key components in atmospheric nucleation, but other stabilizing species are needed to participate in the process to explain atmospheric nucleation. The identity of these species and the mechanisms of the process itself have been elusive. This thesis aims to gain insight on the species participating nucleation and the mechanism of the whole process.

This thesis concentrates first to identify meteorological parameters controlling the atmospheric new particle formation. The information gathered from the field is used to design laboratory experiments more precise for the purpose of studying nucleation. The laboratory experiments were carried out using different flow tubes, first to test the limits of the Classical Nucleation Theory and later on to investigate sulphuric acid-water binary and sulphuric acid-water-base compound ternary nucleation. The precursor gas species were measured using mass spectrometers and ion chromatographs. The measured concentration of sulphuric acid from gas and particle phases were compared to theoretical prediction. The magnitude of the effect of base compounds on nucleation was estimated. The clustering of sulphuric acid molecules with other species was detected. Initial growth of clusters were studied in the point of view of sulphate containing species.

The results from the laboratory experiments confirmed earlier results found in the literature that base compounds increase nucleation rates significantly. The measurements of the gas-phase concentrations of these compounds set an upper limit, where the increasing effect is saturated. Comparison of the sulphuric acid concentrations measured with different techniques and with the theoretical approach showed order-of-magnitude discrepancy. The discrepancy was found to be due to clustering of sulphuric acid molecules with various species. Sulphate-containing species was found to be responsible of the initial growth of clusters in the flow tube measurements. Even though the species participating nucleation are still an open question, the work done in this thesis has helped to identify few of these species and the magnitude of their effect on nucleation. This thesis also helps to understand the initial growth of clusters in flow tube experiments and to identify possible limitation on instruments used commonly in atmospheric measurements.

Keywords: nucleation, atmospheric aerosols, sulphuric acid, flow tube, amines

Contents

List of publications

This thesis consists of an introductory review, followed by five research articles. In the introductory part, the papers are cited according to their roman numerals. **Papers I, III** and **V** are reproduced under the Creative Common License. **Paper II** is reproduced with permission from The Journal of Chemical Physics. Copyright 2014, AIP Publishing LLC. **Paper IV** is reproduced with permission.

I **Neitola, K**., Asmi, E., Hyvärinen, A.-P., Raatikainen, T., Panwar, T.S., Sharma, V.P. and Lihavainen H. (2011) New particle formation infrequently observed in Himalayan foothills – why? Atmos. Chem. Phys., 11, 8447–8458.

II Görke, H., **Neitola, K.**, Hyvärinen, A.-P., Lihavainen H., Wölk, J., Strey, R. and Brus, D. (2014) Homogenous nucleation rates of n-propanol measured in the Laminar Flow Diffusion Chamber at different total pressures. J. Chem. Phys., 140, 174301.

III Brus, D., **Neitola, K**., Hyvärinen, A.-P., Petäjä, T., Vanhanen, J., Sipilä, M., Paasonen, P., Kulmala, M. and Lihavainen, H. (2011) Homogenous nucleation of sulfuric acid and water at close to atmospherically relevant conditions. Atmos. Chem. Phys., 11, 5277–5287.

IV **Neitola, K**., Brus, D., Makkonen, U., Sipilä, M., Lihavainen H. and Kulmala M. (2014) Effect of addition of four base compounds on sulphuric-acid–water new-particle formation: a laboratory study. Boreal Env. Res., 19 (suppl. B): 257–274.

V **Neitola, K.**, Brus, D., Makkonen, U., Sipilä, M., Mauldin III, R.L., Sarnela, N., Jokinen, T., Lihavainen H. and Kulmala, M. (2015) Total sulphate vs. sulphuric acid monomer in nucleation studies, Atmos. Chem. Phys., 15, 3429-3443.

1 Introduction

An aerosol is defined as a mixture of solid or liquid particles suspended in a gas. The concentration and size of atmospheric aerosol particles are very diverse. The number concentration ranges from a few particles per cubic centimetre in Antarctica (Shaw, 1988; Weller et al., 2011; Järvinen et al., 2013) up to several hundreds of thousands per cubic centimetre in heavily polluted urban areas (Mönkkönen et al., 2005; Apte et al., 2011; Guo et al., 2014). The size of aerosol particles ranges from molecular clusters with a diameter of approximately 1 nm, up to cloud droplets or dust particles with a diameter up to hundreds of micrometres. The residence time of particles in the atmosphere range from a few hours to a few weeks, making long transport possible. Aerosol particles can be divided into primary and secondary particles. Primary particles are emitted into the atmosphere directly, for example as dust, spores, sea salt particles, pollen, airborne viruses and bacteria, soot, and smoke. Secondary particles are formed from atmospheric gases via gas-to-particle phase transition. Both primary and secondary particles can be produced by natural or anthropogenic emissions.

Aerosol particles can alter the radiative balance of the Earth's atmosphere by scattering and absorbing incoming solar radiation, which is called a direct effect (Twomey, 1991; Seinfeld and Pandis, 1998), or by acting as cloud condensation nuclei (CCNs), which may alter the albedo and lifetime of clouds, called an indirect effect (Twomey, 1974; Lohmann and Feichter, 2005). According to the Intergovernmental Panel on Climate Change (IPCC), advances have been made recently to understand the effects of aerosol particles, but aerosols continue to contribute the largest uncertainty to the climate forcing estimates (IPCC, 2013). The overall radiative forcing caused by aerosols (cooling) is estimated to be -0.9 (-1.9 to -0.1) W m^{-2} with a medium confidence (IPCC, 2013). The net radiative forcing due to well-mixed greenhouse gases (warming) is estimated to be 2.83 (2.54 to 3.12) W m^{-2}, suggesting that the counteraction by aerosols ranges from negligible to more than half of the warming caused by greenhouse gases (IPCC, 2013).

Nucleation is the initial step in secondary particle formation (Kulmala, 2003; Seinfeld and Pandis, 1998). In nucleation, the supersaturated precursor vapour(s) molecules collide and form small, thermodynamically stable clusters. Nucleation can be divided into homogeneous and heterogeneous nucleation. Homogeneous nucleation occurs without any surface and heterogeneous nucleation occurs on a pre-existing surface. Heterogeneous nucleation has typically a lower energy barrier to overcome (e.g. Winkler, et al., 2008a), and is favoured over homogeneous nucleation in the presence of any surface. The nucleation step is suppressed by the thermodynamic instability of the small clusters of few molecules. The vapour's ability to form critically sized clusters that can grow via condensation depends strongly on temperature, supersaturation and other system parameters. The number of precursor gases participating in the nucleation process can vary. Nucleation with one gas is called unary (homomolecular) nucleation, while it is called binary or ternary nucleation with two and three gases respectively. An even higher number of species is also possible.

Secondary particle formation, or new particle formation, has been observed all around the world and it can be a frequent phenomenon (Kulmala et al., 2004b). Anthropogenic emissions may alter the aerosol particle composition and concentrations, which can affect large populations in sensitive regions. One example of this type of regions is the Himalayas, which is sensitive due to strong regional climate feedbacks. Changes in precipitation patterns and melting of the glaciers could potentially affect more than a billion people on the Indian subcontinent (Menon et al., 2002).

New particle formation events start with nucleation of very small clusters, followed by subsequent condensational growth. The condensing vapours may take part in the nucleation itself, such as with ammonia (Smith et al., 2005) or organics (O'dowd et al., 2002a), or just on the growth. Typical growth rates of freshly formed particles are in the order of a few nm h^{-1} (Kulmala et al., 2004b) but can exceed some tens of nm h^{-1} in highly polluted urban areas (Iida et al., 2008) or even 200 nm h^{-1} (Kulmala et al., 2004b). Particles can also grow by coagulation, where particles collide and stick to each other. Coagulational scavenging into a pre-existing aerosol population is the most important sink for freshly formed particles (Kerminen et al., 2001). New particle formation events can contribute substantially to CCN (Lihavainen, et al., 2003; Merikanto et al., 2009).

Nucleation has been studied intensively for the last few decades, but the underlying mechanism is yet to be solved. Sulphuric acid has been observed to play a key role in atmospheric nucleation (Kulmala et al., 2006; Riipinen et al., 2007; Sipilä et al., 2010; Kirkby et al., 2011). Several different nucleation mechanisms have been suggested for the nucleation that occurs in the atmosphere, including binary nucleation of sulphuric acid and water (Vehkamäki et al., 2002; Yu, 2006; Kirkby et al., 2011), ternary nucleation involving also ammonia and/or amines (Ball et al., 1999; Korhonen et al., 1999; Napari et al., 2002; Benson et al., 2009; Berndt et al., 2010; Kirkby et al., 2011; Zollner at al., 2012) and ion-induced nucleation (Lee et al., 2003; Lovejoy et al., 2004; Yu et al., 2008, 2010; Nieminen et al., 2011). Ions have been shown to lower the thermodynamic potential of nucleation (Arnold 1980; Winkler et al., 2008; Kirkby et al, 2011), but the role of ions in nucleation occurring in the atmospheric boundary layer has been shown to be minor (Manninen et al., 2010; Paasonen, et al., 2010; Kerminen et al., 2010; Hirsikko et al., 2011). Despite the numerous field measurements, laboratory studies and computer simulations, atmospheric nucleation and the species involved in it remain unclear.

The aim of this thesis is to gain further insight into atmospheric nucleation, the initial growth of freshly formed particles, and the species involved in both nucleation and early growth, by direct measurements mainly in the laboratory but also in the field. To achieve this, three main goals were set:

I Characterize new particle formation events and their connection to the boundary layer evolution in the foothills of the Himalayas (**paper I**)

II To gain insight into unary, binary and ternary nucleation mechanisms by means of laboratory experiments, including (**Papers II-IV**)

a. To confirm that the carrier gas pressure effect of unary nucleation of n-alcohols measured using a Laminar Flow Diffusion Chamber (LFDC) depends on the carbon chain length of the n-alcohol

b. To investigate binary H_2SO_4-H_2O and ternary H_2SO_4-H_2O-base nucleation with a laminar flow tube in atmospheric conditions

III To establish the reason behind the discrepancy between measured total-sulphate and sulphuric-acid monomer concentration with two independent sulphuric-acid detection methods, and to study the implication of the discrepancy on the early growth of freshly formed particles (**Paper V**).

2 Materials and methods

The main instruments, d data-analysis methods, and theoretical approach used in this thesis are described in this chapter. This work is based on two types of measurements, field measurements (**Paper I**) and laboratory studies (**Papers II-V**). The field measurements were conducted in Mukteshwar, India, in the foothills of the Himalayan Mountains (Fig. 1). The field study was done to understand the main meteorological and physical parameters controlling atmospheric new particle formation. The knowledge gained from the analysis of new particle formation events was used to concentrate the laboratory experiments towards the most important variables in nucleation.

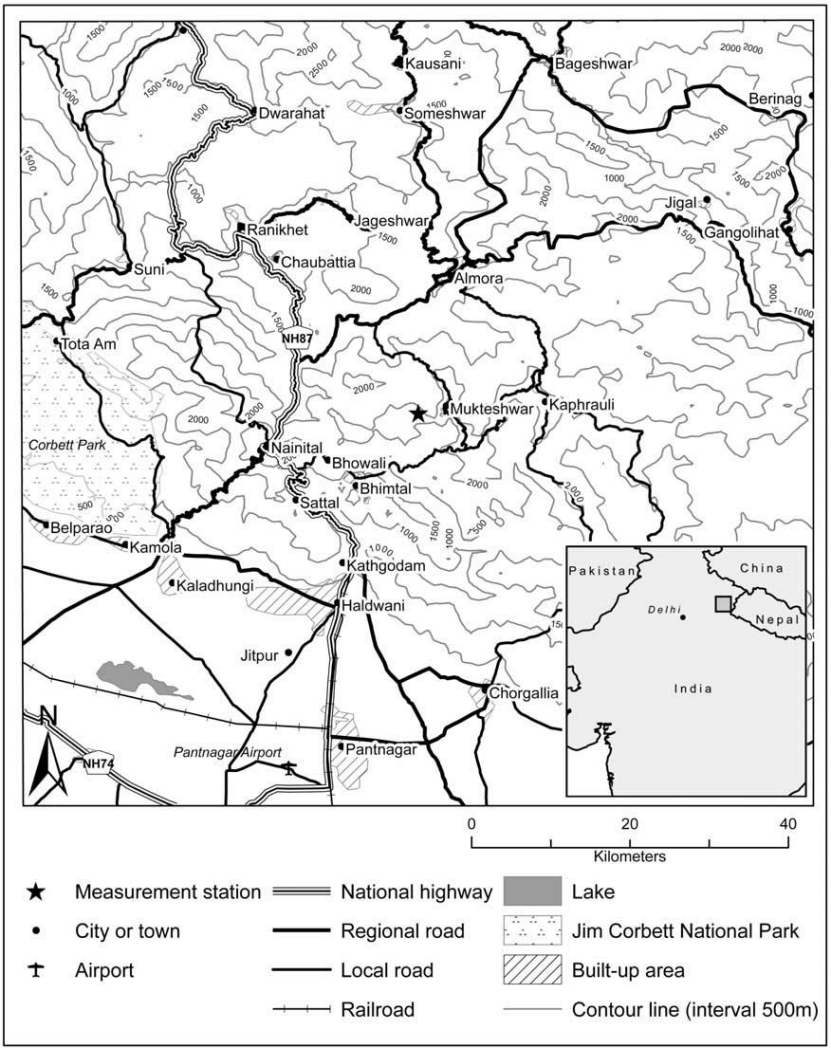

Figure 1. Location of Mukteshwar measurement site, closest towns and some terrain properties. Figure adapted from **Paper I**.

2.1 Instrumentation in the field experiment

Instruments for detecting aerosol particles were similar in the field and in the laboratory. Sulphuric acid vapour concentrations were measured in the laboratory experiments.

2.1.1 Aerosol particle detection

Particle number concentration is typically measured with Condensational Particle Counters (CPC). The condensational detection has been applied since the 19th Century (McMurry, 2000). CPC is an instrument where supersaturated vapour condenses on the particles, growing them to micrometre-size to be individually detected by optical methods. There are several ways to produce the supersaturation of the working fluid (usually alcohol or water): i) conductive cooling of the saturated sample flow (Agarwal and Sem, 1980), ii) turbulent mixing of the saturated warm flow with a colder, sample flow (Kousaka et al., 1982; Sgro and de la Mora, 2004), iii) adiabatic expansion of the sample (Aitken, 1888; Wilson 1897; Winkler et al., 2008a; b) and iv) vapour diffusion from warm wetted walls towards a cooler sample flow (Hering and Stolzenburg, 2005). Commercially available CPCs were used in all of the measurements presented in this work. In **Paper I**, TSI model 3772 CPC was used as a part of the DMPS (Differential Mobility Particle Sizer) system.

The number size distribution below 1 μm is typically measured with a DMPS system. It comprises of a bipolar radioactive neutralizer, Differential Mobility Analyzer (DMA) and a CPC. The particle population in the sample flow is charged (or neutralized) to a known charge equilibrium with the help of ionized molecules of the carrier gas, while the equilibrium charge distribution can be calculated according to the parameterization by Wiedensohler, (1991). Vienna-type DMA (Winklmayer et al., 1991) is used to select a monodisperse (i.e. singly sized) aerosol population from a polydisperse population, with the aid of data inversion according to Stolzenburg (1988). The diameter of the particles in a DMA-segregated monodisperse population is called the electrical mobility equivalent diameter, as differently shaped particles might have the same electrical mobility (Baron and Willeke, 2001). All diameters presented in this work are electrical mobility equivalent diameters. A DMPS system was used to measure the number size distribution in a size range from 10 nm to 800 nm (**Paper I**) in a closed-loop arrangement (Jokinen and Mäkelä, 1997). The dry size of particles was measured in the field measurements (**Paper I**) to eliminate the effect of changing ambient relative humidity (RH) on particle size.

2.2 Data analysis of field experiment

The classification of the New Particle Formation (NPF) events and how the growth rates (GR) and formation rates (FR) are calculated are explained in this chapter. Also, the methodology for determining the Planetary Boundary Layer (PBL) evolution and modelling the trajectories is explained.

2.2.1 Analysis of the NPF events

Formation of new particles in the lower atmosphere is usually identified from a surface plot, where the particle number size distribution is presented as a function of time (Fig. 2). An NPF event is observed as particles appear in the nucleation mode (< 25 nm), i.e. the smallest size channels of the DMPS system.

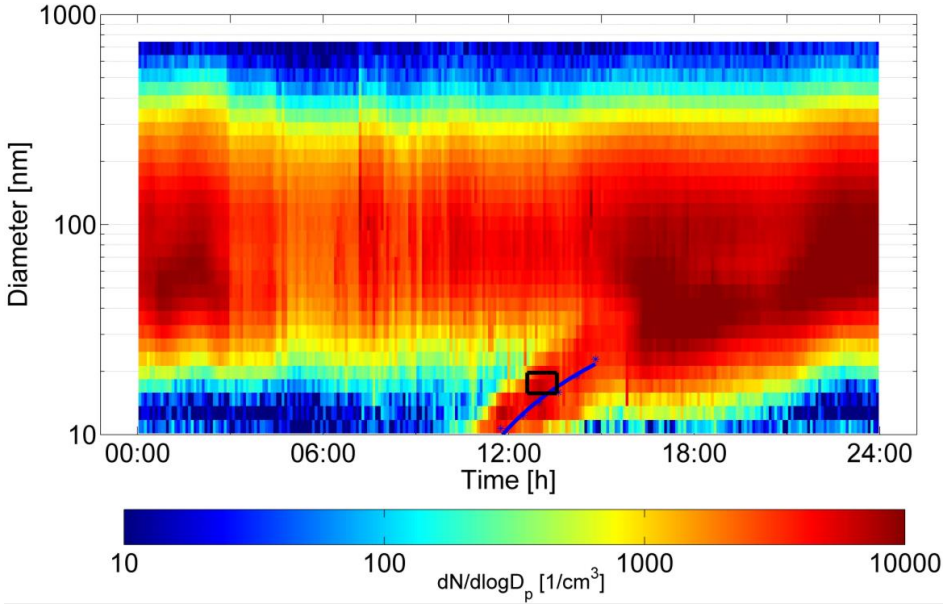

Figure 2. A particle formation event observed on 26 May, 2009. The blue line shows the fitting of growth rate on the data. The 15 nm particle formation rate, J_{15}, was calculated based on data surrounded by the black box. Figure adapted from **Paper I**.

A four-year data set measured in Mukteshwar, India was visually classified on a day-to-day basis following the procedure presented in Mäkelä et al. (2000) and Dal Maso et al. (2005). The days were classified into four classes with the following criteria:

- Class I: Clear NPF event with quantitative growth rate (GR) and formation rate (FR)
- Class II: NPF event but not possible to accurately calculate GR and FR, i.e. possible concentration fluctuations during growth or growth was suppressed
- Class III: Undefined, did not fulfil the characteristics of the event day or a non-event day, for example no clear growth or growing Aitken-mode-sized particles
- Class IV: non-event, no nucleation mode particles

The classification was done independently by two researchers and the results were compared. The days with different classifications ascribed by the researchers were re-examined thoroughly until a consensus was reached.

Particle growth rates (GR) were determined by a visual fitting method (e.g. Kulmala et al., 2001; Hamed et al., 2007). The growth rates were assumed to be constant, thus enabling a linear fit on the median diameter of the nucleation mode visually determined from the figure (blue line in Fig. 2). The growth rates can be also calculated with another method by fitting log-normal modes on each measured nucleation mode particle size distributions and by making a linear fit on the obtained mode median diameters, thus following the procedure by Dal Maso et al. (2005). This was done for five randomly chosen event days (Class I) to ensure the similarity of the results by the two methods. The obtained growth rates were similar, verifying the used method.

The new particle formation rate (FR) was calculated at 15 nm, instead of the smallest measured size of 10 nm, due to decreased measurement precision (diffusion losses, inaccuracy of power supply at low voltages). The determined FR is not the actual nucleation rate, which is the formation rate of critically sized clusters (1-2 nm), but should be considered as an apparent particle formation rate. The actual nucleation rate can be calculated using an analytical tool developed by Kulmala et al. (2001, the so-called Kulmala protocol), where the coagulation sink and growth rate are used to back-calculate the nucleation rate of 1 nm particles. In this method the growth rate is determined from the measured number size distribution and an assumed constant. However, recent studies suggest that the growth rate increases linearly as a function of particle diameter (Kuang et al., 2012). The particle diameter range, from where the growth rate was determined in this study, is above 10 nm, which might lead to an erroneous nucleation rate. The freshly formed particles have been undergoing processes like coagulation, which have affected the concentration and size of the particles before sampling and detection.

The formation rate of 15 nm particles, J_{15} was calculated as

$$J_{15} = \frac{dN_{15-20}}{dt} - CoagS_{17}N_{15-20} - \frac{N_{15-20}}{5\ nm}GR_{15-20}, \quad (2)$$

where the first term is the temporal change of the number concentration N in the size range 15-20 nm, resulting from particle formation. Second term in Eq. (2) describes the coagulation losses, where the coagulation sink, *CoagS*, was calculated as in Kulmala et al. (2001). The wet size of the particles was approximated using the parameterization from Laakso et al. (2004), which is developed for the boreal forest. Even though the chemical species in an aerosol may differ between a boreal forest and the Himalayan foothills, the growth rates reported by Hirsikko et al. (2005) for boreal forest are similar to those found in this study, which supports the use of parameterization. The third term in the Eq. (2) describes the growth of particles out of the size bin used for the determination of the FR (15-20 nm).

2.2.2 Boundary layer evolution and trajectory modelling

To investigate if the NPF events occurred in the free troposphere or in the boundary layer, diurnal evolution of the Planetary Boundary Layer (PBL) height at the station was determined from the European Centre for Medium-Range Weather Forecasts (ECMWF) model,

which runs with 3-h intervals. The PBL heights were calculated as distance weighted averages from the four closest integer coordinate points, i.e. a one-degree resolution.

To gather information on the origin of the air masses and thus on the potential particle sources, the air mass backward trajectories were calculated using a FLEXTRA kinematic trajectory model (Stohl et al., 1995). Trajectories starting every three hours were calculated at the arrival pressure level of 750 hPa and followed 120 hours backwards.

2.3 Instrumentation in the laboratory

Instruments used for particle detection were very similar in the laboratory experiments as those used in the field. Sulphuric-acid production and detection methods as well as the used measurement setups are described.

2.3.1 Particle detection

Similar CPCs were used in the laboratory as in the field. In **Paper II** the particles had already grown to optically detectable sizes, so only the optical-detection part of a TSI model 3010 was used. Several different CPC's were used in **Papers III-V** as a part of a DMPS system and as an individual instrument. The lowest detectable size of a particle (cut-off diameter) depends on many properties of the CPC, though mainly on the temperature difference of the saturator and the condenser, the working fluid used (Iida, et al., 2009), and the composition and the charge of the particles. Commercially available CPCs typically have a cut-off diameter of 3 nm (TSI models 3025A and 3776) or 7 nm (TSI models 3010 and 3772). Recent developments of expansion types (Kürten et al., 2005) and mixing types of CPC (Sgro and de la Mora, 2004) have lowered the cut-off diameter well below 3 nm. One such commercially available instrument is the Particle Size Magnifier (PSM, Airmodus ltd., Finland; Vanhanen et al., 2011), with a cut-off diameter below 1.5 nm. Due to its ability to detect extremely small particles, it is well suited to laboratory nucleation studies (**Papers III-V**), where the particles initially are very small. The working fluid used in PSM (diethylene glycol) has a very low vapour pressure and it is not able to grow the particles to optically detectable sizes, so it must be used in combination with a CPC (TSI model 3772, in this work). The DMPS system measured in the range of 3 nm to some 250 nm (**Papers III-V**) for wet sizes, and it was used to investigate the effect of RH on particle size.

2.3.2 Sulphuric-acid vapour production

Numerous laboratory experiments have been conducted to find out the role of sulphuric acid in atmospheric nucleation (e.g. Viisanen et al., 1997; Ball et al., 1999; Benson et al., 2008, 2011; Young et al., 2008; Berndt et al., 2008, 2010; Brus et al., 2010; Sipilä et al., 2010; Kirkby et al., 2011; Zollner et al., 2012) with different methods to produce the sulphuric-acid vapour for the actual nucleation process. Most common is the gas-phase oxidation of

sulphur dioxide with hydroxyl radicals to produce sulphuric acid, since it is similar to that observed in the atmosphere (Stockwell and Calvert, 1983):

$$SO_2 + OH \rightarrow HOSO_2; HOSO_2 + O_2 \rightarrow HO_2 + SO_3; SO_3 + H_2O \rightarrow H_2SO_4 \quad (1)$$

The oxidation of SO_2 have been used in many experiments (e.g. Benson et al., 2008; Berndt et al., 2008, 2010; Sipilä et al., 2010; Kirkby et al., 2011). The OH radicals are produced with the use of UV-light. The excess OH must be removed to prevent alteration of the nucleation process itself (Berndt et al., 2010). OH radicals can be removed by having an excess of SO_2, but with this method, the calculation of the produced sulphuric acid concentration requires exact knowledge of the OH concentration (Benson et al., 2008). In this work (**Papers III and V**) and in Viisanen et al. (1997), sulphuric acid was produced by evaporation of a weak sulphuric acid-water solution in a furnace. In this method, the sample solution is pumped with a peristaltic pump with a constant rate through a ruby micro-orifice to produce small droplets. The droplets are taken into a heated furnace with a carrier-gas flow, where the droplets are evaporated (**Paper III**). The input of sulphuric acid can be determined from the solution. The disadvantage is a thermal gradient created by the heated furnace, which increases wall losses.

Ball et al. (1999) and Zollner et al. (2012) used a similar sulphuric-acid vapour production method that was used in this work (**Papers IV-V**), by saturating a carrier-gas flow in a thermally controlled saturator. The saturator used in this work was a horizontally placed cylinder made of iron, with a Teflon insert inside the cylinder (inner diameter, I.D. of 5 cm). The temperature of the saturator was measured just above the liquid sulphuric acid with a calibrated PT100 probe (± 0.05 K) inserted from the outlet side of the saturator. The saturator, the inlet and the outlet connected to it were thermally controlled with a circulating liquid bath (LAUDA RC 6). A schematic figure of the saturator-test setup is presented in Fig. 3. The incoming dry carrier-gas flow in the range 0.05–2 litres per minute (lpm) was purified with an activated-carbon capsule (PALL Corp., USA) to remove condensing vapours via diffusion onto the surfaces and with High-efficiency particulate arrestance (HEPA) filters (PALL Corp., USA) to remove particles from the flow. The saturator flow was mixed with another flow, which was purified in the same manner and if necessary, humidified with a set of Nafion humidifiers. This mixing flow was introduced to meet the demanded inlet flows of the instruments used and to dilute the sulphuric acid concentration to the desired levels. Both flow rates were controlled with mass flow controllers to within ±3 % (MKS type 250).

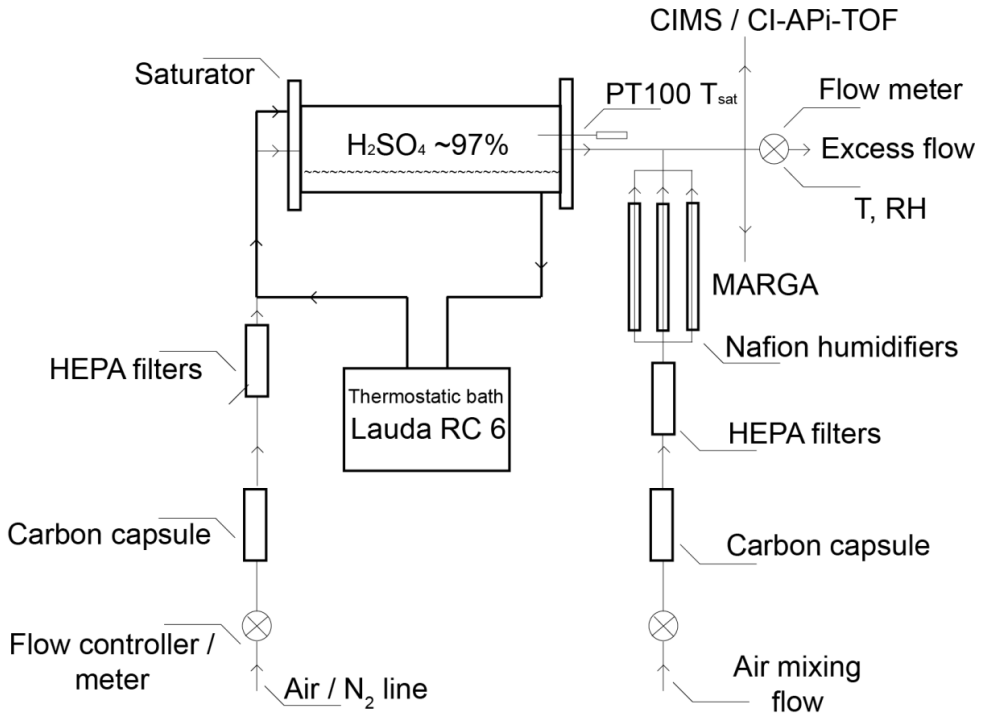

Figure 3. Schematic figure of the setup for testing the saturator. Figure adapted from **Paper V**.

2.3.3 Sulphuric-acid detection

Precise determination of sulphuric-acid concentration is crucial for the prediction of nucleation rates and subsequent growth. Direct detection of gas-phase sulphuric acid was not possible before the early 20th Century, when the Chemical Ionization Mass Spectrometer (CIMS, Eisele and Tanner, 1993; Mauldin et al., 1998; Eisele and Hanson, 2000; Petäjä et al., 2009) was introduced. In some earlier nucleation experiments involving sulphuric acid, the sulphuric-acid concentration was calculated as relative acidity (Wyslouzil et al., 1991) or the sulphuric-acid input was determined (Viisanen et al., 1997).

2.3.3.1 Mass spectrometry

After the introduction of CIMS, the Chemical Ionization Atmospheric Pressure interface Time-of-Flight mass spectrometer was developed (CI-APi-TOF, Tofwerk AG, Thun, Switzerland and Aerodyne Research Inc., USA; Junninen et al., 2010; Jokinen et al., 2012), with a similar Chemical Ionization inlet as the CIMS (Jokinen et al., 2012). Both of these mass spectrometers were used in this work (**Papers III-V**).

The CI-inlet is used to charge the sulphuric-acid molecules (H_2SO_4) via proton transfer with nitrate ions (NO_3^-). The nitrate ions are produced from nitric acid with a radioactive ^{241}Am-source and mixed in a controlled manner in a drift tube, using a concentric sheath and sample

flows together with electrostatic lenses (Jokinen et al., 2012). The chemical ionization is a relatively soft ionization method and it does not dissociate the molecules. Some base molecules might be replaced by the charging ion; for example ammonia may be replaced by the nitric acid molecule in a cluster containing sulphuric acid (Kurten et al., 2011). The proton transfer allows charging of almost any type of molecule that has a smaller proton affinity than the nitrate ion. To be able to determine the actual atmospheric concentration of some species, the charging efficiency must be obtained via a calibration procedure, where a known amount of the species is introduced into the inlet of the instrument.

After the ionization, the two mass spectrometers differ from each other. The sample flow of CIMS is dried with a nitrogen flow to dehydrate the molecules before entering the vacuum system. The Collision Dissociation Chamber (CDC) operates in the vacuum system. A set of resistors forms a repulsive electric field, which weakens as the ions move forward in the vacuum (Petäjä et al., 2009). The ions undergo collisions with the N_2-molecules, leaving the core ions (NO^-_3 and HSO^-_4) (Eisele, 1986). After the CDC, the ion beam is collimated with conical octopoles and directed to the quadrupole mass spectrometer, where the ions are detected with a channeltron (Petäjä et al., 2009).

In CI-APi-TOF, the sample flow (0.8 lpm) is taken through a critical orifice (300 µm) into a differentially pumped APi. The APi consists of three stages, the first two contain short segmented quadrupoles guiding the ions and the third contains an ion lens assembly (Junninen et al., 2009). The detection of the ions is done with time-of-flight type mass spectrometer in CI-APi-TOF. CI-APi-TOF has higher mass resolution and detection range due to the improved mass spectrometer (Junninen et al., 2009). CI-APi-TOF can be used to detect larger clusters containing solely sulphuric acid (dimer, trimer, etc.) or a combination of different species (Jokinen et al., 2012).

The actual concentration of sulphuric acid monomer in the sample flow is determined with the ratio of the sum of the resulting ion signals (HSO_4^- and $HSO_4^-{\cdot}HNO_3$) and the reagent ion signals (NO_3^-, $HNO_3{\cdot}NO_3^-$ and $(HNO_3)_2{\cdot}NO_3^-$). The ratio is multiplied with an instrument-dependent factor, which is determined by calibration of the instrument. The standard calibration procedure of CIMS is done by oxidation of SO_2 with OH radicals, produced with photolysis of water with UV light. The resulting H_2SO_4 concentration is calculated with a numerical model. For more detailed description of the calibration procedure, please see Berresheim et al. (2000), Petäjä et al. (2009), Zheng et al. (2010), and Kürten et al. (2012).

2.3.3.2 Ion Chromatography

Ion chromatography is a technique used to separate ions or polar molecules based on their ionic (coulombic) forces. The ions of the species measured (from the gas and aerosol phase, in our case) are produced within the absorbance solution and internal standard. The detection of different species is based on their conductivity.

Two different types of ion-chromatography methods were used in this work. First an offline method of bubblers, where a known sample flow rate is bubbled through an alkaline solution for a known period of time, trapping all the sulphate (Brus et al., 2010), was used. The

solution was later analysed with an ion chromatograph. The bubbler traps particles as well as gas phase sulphuric acid. The ion chromatograph detects the sulphuric acid as sulphate ions (SO_4^{2-}), thus the expression sulphate is used in this work when considering sulphuric acid detected with an ion chromatograph. The source of sulphate in this work was always the sulphuric acid vapour used to produce the particles. The sources of sulphate in the atmosphere are more versatile and cannot be deduced to originate only from sulphuric acid vapour. The concentration of sulphate in the sample flow was determined from the resulting concentration in the alkaline solution with the help of the known flow rate and bubbling time.

The second method involved an online ion chromatograph, which is an instrument for measuring aerosols and gases (MARGA 2S ADI 2080, Metrohm applikon analytical BV, Netherlands; ten Brink et al., 2007) that is analogous to the bubbler method. According to the manufacturer, MARGA is able to detect five species in the gas phase (HCl, HNO_3, HONO, NH_3 and SO_2) and eight major inorganic species from the particle phase (Cl^-, NO_3^-, SO_4^{2-}, NH_4^+, Na^+, K^+, Mg^{2+} and Ca^{2+}). A high inlet flow rate (1 m^3 h^{-1}) minimises the losses in the sampling lines. MARGA separates the particle and gas phases with two separate collection stages; from the sample flow, all (99.7 %) water soluble gases are absorbed into a wetted rotating denuder (WRD). Based on the different diffusion velocities, particles pass the WRD and enter the steam-jet-aerosol collector (SJAC; Slanina et al., 2001). Conditions in the SJAC are supersaturated with respect to water vapour, which condenses on the particles. The particles grow until they are collected on the bottom of the SJAC. Sample solutions are drawn once an hour from the WRD and SJAC for the ion chromatograph to be analysed. Different species are detected by conductivity measurements and the detection limits are 0.1 µg m^{-3}, or better.

The separation by diffusion velocities between particles and gas phase can function better for larger particles. In nucleation studies, where particles are usually very small in diameter (some tens of nanometres or smaller), diffusion velocities between gas phase and particles are of a similar order and the separation does not function well. Due to this, only total sulphate (gas + particle phase) is reported in this work. This also enables a direct comparison with the bubbler method, where gas and particle phases were not separated. MARGA can be used to detect other species than those reported by the manufacturer (for example amines) by first calibrating the instrument by injecting a known concentration of the species directly into the ion chromatograph for it to identify the conductivity peak produced by this species.

2.3.4 Laminar flow diffusion chamber

An inert carrier gas has been used in unary homogeneous nucleation studies mainly as a latent heat reservoir, i.e. maintaining isothermal conditions (e.g. Wyslouzil and Seinfeld, 1992) and typically the existence of the carrier gas has been neglected. However, experimental studies of the unary homogeneous nucleation of n-alcohol (Hyvärinen et al., 2006, 2008; Brus et al., 2006, 2008) as well as water (Hyvärinen et al., 2010) strongly suggest a

dependence of the carrier gas pressure on the nucleation rate. To extend the data set measured with a Laminar Flow Diffusion Chamber (LFDC) for n-butanol (Hyvärinen et al., 2006, 2008) and n-pentanol (Brus et al., 2008), the isothermal nucleation rates of n-propanol were measured as a function of supersaturation at various temperatures and pressures (**Paper II**).

The LFDC used in this work was originally set up by Lihavainen and Viisanen (2001). The main principle is to saturate an inert carrier gas in a horizontally placed, thermally controlled saturator, which is half filled with the nucleating substance. The gas-vapour mixture is taken into a preheater and a condenser, which are vertically placed co-axial tubes with the same inner diameter. A preheater is kept at higher temperature than the saturator to prevent condensation and assure laminar flow with a known velocity profile. After the preheater, the flow enters the condenser, which is at a much cooler temperature than the preheater. The almost stepwise temperature change increases the saturation ratio of the vapour above the critical saturation ratio, leading to nucleation and subsequent growth of the particles up to optically detectable sizes. The particles were detected in this study at the end of the tube with an optical cell. The obtained nucleation rates were compared to a theoretical prediction by Wedekind et al. (2008), which incorporates the carrier gas pressure dependency into Classical Nucleation Theory (CNT, Becker and Döring, 1935).

2.3.5 Laminar flow tube

Binary and ternary homogeneous nucleation measurements in this work (**Papers III-V**) were carried out using a laminar flow tube originally presented in Brus et al. (2010). The laminar flow tube was more suitable for experiments with sulphuric acid vapour due to the mixing unit design and the larger volume of the tube, increasing usable residence time, than the LFDC. A schematic figure of the setup is presented in Fig. 4 with the saturator as a source of the sulphuric-acid vapour. The setup consists of four main components: sulphuric acid production, a mixing unit, a laminar-flow nucleation chamber, and detection of particles and sulphuric acid vapour or total sulphate. The flow with the sulphuric acid vapour (produced as described in section 2.1.2) is turbulently mixed with a dry, clean, particle-free carrier gas in the mixing unit. After the mixing unit, a third compound (e.g., amine, ammonia) can be added to the flow before the nucleation and subsequent growth takes place in the thermally controlled laminar-flow nucleation chamber. The freshly formed particles and sulphuric acid vapour or total sulphate are detected immediately at the end of the flow tube. The flow tube itself consists of two 100 cm-long stainless steel cylinders (I.D. 6 cm) connected with a Teflon piece (height 3.5 cm, I.D. 6 cm). One of the 100 cm-long cylinders has four holes on the sides every 20 cm from the beginning of the cylinder. The Teflon piece connecting the cylinders also has a hole (see Fig. 4). These holes are used to continuously monitor the temperature of the flow tube with calibrated PT100 probes to ensure desired nucleation temperature. The RH of the mixing flow was set with Nafion humidifiers and measured together with the temperature from the excess flow at the end of the flow tube. The typical flow rate in the tube was ~11 lpm, which results in a residence time of 30 s (plug flow). Varying the mixing flow rate, the residence time varied between 30 and 90 s.

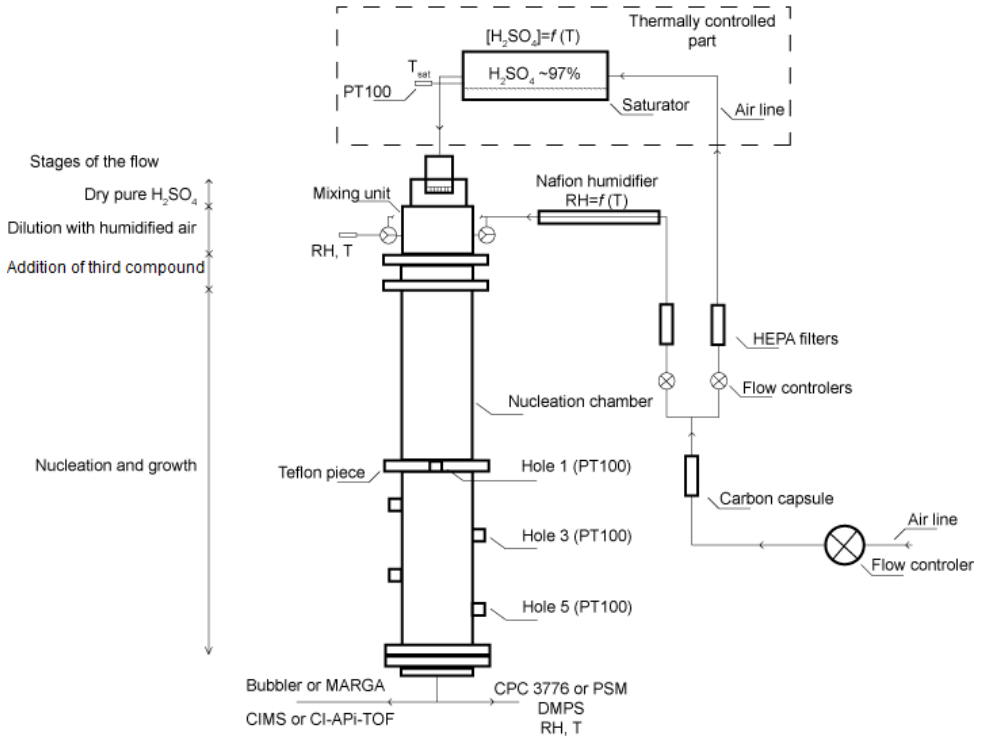

Figure 4. A schematic figure of the setup for binary and ternary nucleation experiments with a saturator as the source of sulphuric acid vapour. Figure adapted from **Paper V**.

2.4 Theoretical approach for interpretation of laboratory results

Two separate theoretical approaches were used to interpret the results. The first considers the vapour pressure of sulphuric acid, which was used to predict the sulphuric-acid-vapour concentration from the saturator to compare the measured values to the theoretical ones. The second theoretical approach was adapted from Wedekind et al. (2008), where theoretical corrections were made to the CNT as a result of the amount of the carrier gas in homogeneous nucleation studies. The experimental values were compared to theoretical ones. The kinetic (McCurry, 1980) and activation model (Kulmala et al., 2006) for the formation rate of neutral particle dependence on the sulphuric acid concentration is presented.

2.4.1 Vapour pressure of sulphuric acid

The saturator method enables the prediction of sulphuric-acid concentration from the saturation vapour pressure of sulphuric acid and a mixing law. The theoretical output of the saturator was calculated using the equation for the saturation vapour pressure of sulphuric acid by Kulmala and Laaksonen (1990), where the measurements by Ayers et al. (1980) were extrapolated to a lower temperature range:

$$\ln p = \ln p_0 + \frac{\Delta H_v(T_0)}{R} \times \left[-\frac{1}{T} + \frac{1}{T_0} + \frac{0.38}{T_c - T_0} \times \left(1 + ln\frac{T_0}{T} - \frac{T_0}{T} \right) \right], \quad (3)$$

where p is the saturation vapour pressure (atm), p_0 = -(10156 / T_0) + 16.259 atm (Ayers et al., (1980), T is the temperature, T_c is the critical temperature (905 K), T_0 is chosen to be 360 K so that ΔH_v (T_0) / R = 10156. See Kulmala and Laaksonen for more details. The output of the saturator was predicted also with an equation by Richardson et al. (1986), which is a fit to their experimental data in the temperature range 263.15 K – 303.15 K:

$$\ln p = 20.70 - \frac{9360}{T}, \quad (4)$$

where p is the saturation vapour pressure and T is the temperature. When calculating the prediction of sulphuric-acid concentration with the Eqs. (3) and (4), the only variables are the temperature of the saturator, the saturator flow rate, and the mixing flow rate.

2.4.2 Carrier gas pressure correction for the CNT

The existence of the inert carrier gas is usually neglected in homogeneous nucleation studies and it is usually used as a latent heat reservoir. Wedekind et al. (2008) made corrections to the CNT, where the extremes of carrier gas amounts were taken into account. Too high an amount of carrier gas leads to additional volume work, which inhibits the cluster formation. In CNT the formation free energy has a maximum at the critical cluster size n^* and its height ΔG^* is

$$\Delta G^* = \frac{16\pi}{3} \frac{v_l^2 \gamma^2}{\Delta\mu^2}, \quad (5)$$

Where v_l is the volume per molecule in the bulk liquid, γ is the surface tension and $\Delta\mu$ is the difference in chemical potential between liquid and vapour. The isothermal steady-state nucleation rate is

$$J_{CNT} = K\exp\left(\frac{\Delta G^*}{k_B T}\right), \quad (6)$$

Where K is a kinetic prefactor. The difference in chemical potential is given by

$$\Delta\mu = k_B T \ln S - v_l\left(p - p_{\mathrm{eq}}\right), \quad (7)$$

Where S is the supersaturation and p_{eq} is the equilibrium vapour pressure. The second term in Eq. (7) describes the pressure-volume work the droplet has to perform on the vapour pressure (Reguera et al., 2003). The droplet has to perform pV-work against the carrier-gas pressure also, which can be placed inside an "effective chemical potential"

$$\Delta\mu_{eff} = k_B T \ln S - v_l\left(p + p_c - p_{\mathrm{eq}}\right). \quad (8)$$

Here the p_c is the pressure of the carrier gas. Inserting Eq. (8) to Eq. (5) and finally to Eq. (6) gives the pV-corrected nucleation rate

$$J_{pV} = K\exp\left(\frac{G^*_{pV}}{k_B T}\right), \quad (9)$$

A low amount of carrier gas might lead to non-isothermal conditions as the thermalization might not be perfect. Physically the thermalization is a competition between the latent heat energy increase and the energy removal by elastic collisions with the vapour and the carrier gas. The amount of energy released by a monomer addition to a cluster, with a latent heat *h* per molecule, can be expressed with a parameter

$$q = h - \frac{k_B T}{2} - \gamma \frac{dA(n)}{dn}, \tag{10}$$

Where the second term is a small correction to the latent heat and the last term is the energy needed to increase the surface area *A*. The mean squared energy removed by collisions with the impinging molecules is

$$b^2 = 2k_B^2 T^2 \left(1 + \frac{N_c}{N}\sqrt{\frac{m}{m_c}}\right), \tag{11}$$

where *m* is the molecular mass and *N* the number of molecules in the condensable (Wedekind et al., 2007). Combining Eqs. (10) and (11) we get the nonisothermal effects on the steady-state nucleation rate:

$$J_{\text{nonisoth.}} = \frac{b^2}{b^2+q^2} J_{\text{isoth.}}. \tag{12}$$

To get the full pressure-effect (PE) on the nucleation rate, we combing Eqs. (9) and (12)

$$J_{\text{PE}} = \frac{b^2}{b^2+q^2} J_{pV}. \tag{13}$$

The experimental and theoretical nucleation rates were normalised with the theoretical prediction from CNT and plotted as a function of the ratio of partial pressures of the carrier gas and nucleating vapour so as to be able to compare the effect of the carrier gas pressure only.

2.4.3 Formation rate dependence on the sulphuric acid concentration

The vapour concentration of sulphuric acid has been connected to atmospheric new particle formation by many studies (e.g. Weber et al., 1996, 1997; Kulmala, 2003; Riipinen et al., 2007). The formation rate of neutral particles dependence on the sulphuric acid can generally be expressed with two models, the kinetic model (McMurry, 1980) and the activation model (Kulmala et al., 2006). Parameters for both models are determined from atmospheric data, where gas phase sulphuric acid has been measured with similar CIMS, as introduced in chapter 2.1.3.1, and the particle concentration measured with ultrafine particle counters. The activation model has a quadratic and kinetic model linear dependence on the sulphuric acid concentration. The models can be expressed in the form of:

$$J = (K \; or \; A) \times [H_2SO_4]^E \tag{14}$$

Where *K* is a kinetic coefficient with a range between 10^{-14}-10^{-11} cm^{-3} s^{-1} and *A* is an activation coefficient with a range between 10^{-7}-10^{-5} s^{-1} (e.g. Weber et al., 1996; Vehkamäki et al., 2002; Sihto et al., 2006; Riipinen et al., 2007; Kuang et al., 2008; Paasonen et al., 2010), *E* is an exponent, which has been thought to be associated with the number of sulphuric acid

molecules in a critical cluster (Kashchiev, 1982), which is found to be between 1 and 2 when determined from atmospheric measurements.

2.5 Limitation of the measurement setups and instruments

The experiments in this thesis are very different from each other regarding the environment and instrumentation. The conditions in the field are not controlled, which makes data analysis and drawing valid conclusions harder, as many variables may be changing during one measurement cycle. Also, measuring all the important variables is impossible in the field. In the laboratory, conditions such as temperature, relative humidity, etc. can be controlled, which is why nucleation experiments are usually done in the laboratory.

In **Paper II**, the most crucial parameter to control is temperature. A slight change in temperature changes the supersaturation, which can change the nucleation rate by many orders of magnitude. With the stepwise temperature change used in **Paper II**, the flooding of the particle detector was also an issue that limited the usable pressure range.

The largest source of error and the most complicated issue in **Papers III-V** was the detection of sulphuric acid. Sulphuric acid is very "sticky", i.e. once in contact with any surface, it stays on the surface. Sulphuric acid was also present in many different forms, in the gas phase as sulphuric acid and in molecular clusters containing other species also, which complicated the detection with mass spectrometers. The vapour pressure of sulphuric acid is extremely low, causing it to condense on particles, decreasing the gas-phase concentration. Measuring the concentration of sulphuric acid in the particles was not possible with the instrumentation available, so assumptions and higher limits of the amount in the particles had to be applied. The ion chromatographic method to detect sulphuric acid covers all forms of sulphuric acid, but as it is detected as a sulphate, other possible sources of sulphate might cause erroneous results. To minimize this error, the background level of sulphate was measured and taken into account.

Nucleation is extremely sensitive to the levels of contaminants. The carrier gas and the water used for humidifying the carrier gas was the largest source of impurities in the laboratory experiments. Several different cleansing techniques were used to clean the carrier gas but it is impossible to remove all contaminants. The level of contaminants was at an acceptable level, as it was similar as most important studies found in literature. The lower detection limit of the ion chromatographs sets the limit of detection for different contaminant species.

The experiments and the associated data analysis were done with extreme caution and in the best possible way with the instruments available and I am confident that the results are of high quality, given the above-mentioned limitations.

3 Results and discussion

This section is divided according to the nature of the measurements, i.e. field or laboratory studies. The study concerning the discrepancy of the measured sulphuric acid monomer and total sulphate concentrations is separated.

3.1 Characteristics of NPF events in the foothills of the Himalayas

NPF events were observed in 11.2 % of the days with applicable data in **Paper I**. 77.5 % of the days were classified as non-event days and the rest as undefined days. The overall event-to-non-event ratio was 14.5 %, which is relatively low compared to the ratio of 45.2 % measured in boreal forest, Southern Finland (Dal Maso et al., 2005). The seasonality of the NPF event days was strongly pronounced, with 81.5 % of the event days occurring during spring (March–June).

The main characteristics of new particle formation are the growth and formation rates. The growth rate is mainly determined by the concentration and properties of condensable vapours (Kulmala, 1988). The growth rates observed can range from 0.1 nm h^{-1} in clean polar areas, up to 200 nm h^{-1} at coastal sites (Kulmala et al., 2004b); typically, though, growth rates vary in the range of 1–20 nm h^{-1}. The seasonal observed growth rates in the Himalayan foothills (**Paper I**) were found to be in the range of 1.45–3.1 nm h^{-1}, with the minimum found during autumn (mid Sep – end of Nov) and the maximum during winter (Dec – end of Feb), which is similar to some other high altitude sites (e.g. Venzac, et al., 2008; Nishita et al., 2008).

The formation rates reported in the literature vary considerably, with typical formation rates of 3 nm particles within a range of 0.01 to 10 cm^{-3} s^{-1} (Kulmala et al., 2004b). Formation rates have been observed to exceed these typical ranges in some heavily polluted urban sites (Mönkkönen et al., 2005; Wu et al., 2007; Xiao et al., 2015). The apparent formation rates J_{15} reported in **Paper I** range from 0.14 cm^{-3} s^{-1} (autumn) to 0.44 cm^{-3} s^{-1} (spring), with a mean value of 0.4 cm^{-3} s^{-1}.

It has been suggested that atmospheric new particle formation is either suppressed or strengthened by meteorological conditions (e.g. Komppula et al., 2003; Riipinen et al., 2007; Dal Maso et al., 2007). One major condition is the amount of solar radiation, which promotes the photochemical oxidation processes. Radiation also increases the vertical mixing of the atmosphere, diluting the condensational sink (CS, e.g. Kulmala et al., 2001). Increased relative humidity can suppress the growth of freshly formed particles due to wet scavenging of the particles and precursor gases (Hamed et al., 2007).

The strong seasonality of the NPF events observed in **Paper I** was connected with meteorological conditions and diurnal boundary layer evolution. Higher solar radiation during spring (mean global irradiance 203.4 W m^{-2}) not only increased the photochemical oxidation processes but also increased the height of the planetary boundary layer (PBL) by warming

the surface air, causing the air to rise. Under favourable meteorological conditions, the top of the PBL was able to reach the height of the station (2180 m.a.s.l.), which further enabled the transport of particle precursor gases from lower altitudes to the station (Raatikainen et al., 2011). Similar NPF–event dependence on the PBL evolution has been reported in the literature (Venzac et al., 2008; García et al., 2014). The pronounced amount of NPF events in spring can be considered to be a combination of increased solar irradiance, which is diminished during summer due to the monsoon, and the evolution of the PBL. A similar effect from reduced solar irradiance on the NPF event occurrence during the monsoon season was found also by Venzac et al. (2008). The modelled height of the PBL layer was found to reach the station altitude prior the apparent start time of the NPF events during spring. Note that here the start time of the NPF event is defined as time when it is observed at 15 nm at the station. The mean height of the PBL was 2600 m.a.s.l. at the average start time of the NPF events, in contrast to the non-event days, when the average PBL height was below 1500 m.a.s.l. Most of the observed NPF events during spring can be considered happening in the boundary layer, but the sporadic NPF events observed outside spring were taking place in the free troposphere due to the much lower PBL height (1200 m.a.s.l.). However, PBL reaching the station does not solely necessitate an NPF event, suggesting a dependence on other meteorological variables too.

3.2 Laboratory nucleation experiments

The nucleation experiments for this work (**Papers II-V**) were done in the Finnish Meteorological Institute using two different flow devices presented in sections 2.1.4 and 2.1.5. All conducted experiments were homogeneous nucleation experiments, i.e. vapour-to-liquid phase transition without pre-existing aerosols.

3.2.1 Carrier gas pressure effect on homogeneous nucleation of n-propanol

Classical Nucleation Theory (CNT, Becker and Döring, 1935) is the simplest thermodynamic theory for predicting isothermal nucleation rates as a function of saturation ratio. CNT often fails to predict the experimental nucleation rates by up to several orders of magnitude, depending on the nucleating substance (Ford et al., 2004). CNT assumes that properties like surface tension, density and equilibrium vapour pressure have similar values for the microscopic clusters and particles as measured in the bulk phase. As the surface-to-volume ratio is much larger for the clusters compared to the bulk phase, this assumption fails. While enhancements in theories assimilate the surface tension and droplet curvature into the cluster size (Kalikmanov et al., 2006; Oxtoby and Evans, 1988; Napari and Laaksonen, 2007; Soek and Oxtoby, 1998), for molecules that cannot be simply described by intermolecular potentials, the physical properties of a microscopic cluster remains inaccessible. For this reason, predictions by CNT are mostly used as a reference value when comparing experimental and theoretical values.

Since earlier studies show good agreement of theoretical predictions and experimental results of n-alcohol nucleation rates (Strey et al., 1986a, 1986b), isothermal nucleation rates of n-propanol in helium were measured as a function of supersaturation at several temperatures and pressures to extend the former Laminar Flow Diffusion Chamber (LFDC) measurements for n-butanol (Hyvärinen et al., 2006, 2008) and n-pentanol (Brus et al., 2008) measured in similar conditions. The results were compared to literature values and theoretical prediction and these are summarized here.

Nucleation rates were measured between 10^0 and 10^6 cm^{-3} s^{-1} at nucleation temperatures of between 270 K and 300 K in 10 K steps. Three different amounts of carrier gas were used: under pressure (50 or 60 kPa), ambient pressure (100 kPa), and over pressure (200 kPa). An under pressure of 60 kPa was used for a 300 K-isotherm, as the droplets grew extremely fast, flooding the counting system almost immediately. A positive pressure effect (i.e. increasing nucleation rate with increasing pressure) was observed at lower isotherms, with the largest at 270 K, decreasing as a function of the temperature. The pressure effect was not observed at a nucleation temperature of 300 K.

To further reveal the impact of the carrier gas pressure, another experiment was done where not only the nucleation temperature, but also the saturation ratio was kept constant ($\Delta T = \pm$ 0.05 K, $\Delta S = \pm$ 0.03). The supersaturation was calculated with the numerical model described in Lihavainen (2000). Assumptions used in the model are steady state, incompressible flow, and zero radial velocity (laminar flow), resulting in equations of heat and mass transfer to be solved (Lihavainen, 2000). The model uses thermodynamic properties as an input, as listed in Brus et al. (2006). The observed nucleation rates were normalized with the value measured at an under pressure of 50 kPa to emphasize the trend and magnitude of the pressure effect. The normalized experimental nucleation rates of n-propanol $J_{exp} / J_{exp\ (50\ kPa)}$ as a function of total pressure p_{nuc} at nucleation temperatures of 270 K, 280 K and 290 K are presented in Fig. 5. As seen in Fig. 5, the normalized nucleation rates increase as a function of the carrier gas pressure, with a less pronounced effect at higher pressures. The strongest pressure effect is observed at the lowest temperature of 270 K, with three orders of magnitude difference in nucleation rates.

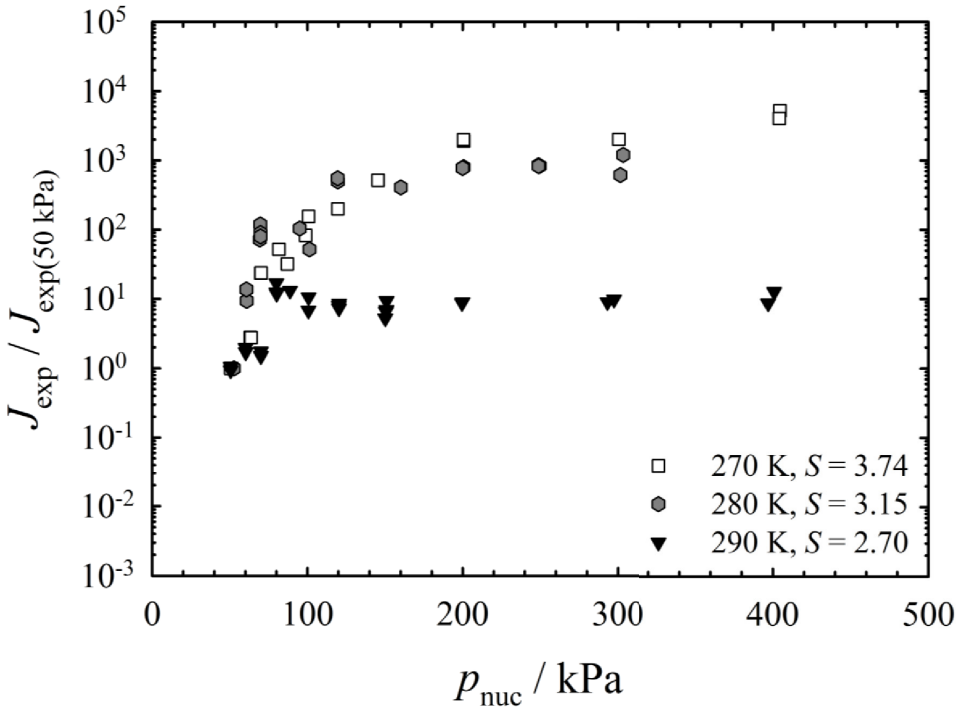

Figure 5. Experimental nucleation rates of *n*–propanol as a function of total pressure for the isotherms at 270 K, 280 K, and 290 K. For each isotherm, the saturation ratio is kept constant. For the sake of comparison, the experimental nucleation rates are normalized by their values obtained at the lowest measureable pressure at 50 kPa. Figure adopted from **Paper II**.

The observed nucleation rates were compared to the CNT and the experimental results fit reasonably well with the theory. At isotherms 290 K and 300 K, experimental values are higher than the prediction by the CNT, whereas at 280 K and 270 K the theory overestimates experimental values. The temperature dependence of the experimental values is stronger than the prediction by the CNT, which has been observed earlier (Wölk and Strey, 2001; Iland et al., 2007; Manka et al., 2010).

Experimental values were also compared to the theoretical approach by Wedekind et al. (2008), where the extremes of carrier gas amounts were taken into account, as explained in chapter 2.3.2.The observed nucleation rates undergo a several orders of magnitude larger pressure effect than that predicted by the theoretical approach, depending on the isotherm considered. The pressures used in this work were in a range where the theoretical approach does not predict a noticeable effect on the nucleation rates. For example, the experimental nucleation rates at a temperature of 270 K increase by 4 orders of magnitude, whereas the theory predicts only an increase of less than half an order of magnitude.

The observed nucleation rates of n-propanol in ambient pressure agree well with other results found in the literature measured with a Thermal Diffusion Cloud Chamber (TDCC, Brus et al., 2006), a Nucleation Pulse Chamber (NPC, Strey et al., 1986b) and a Piston Expansion Tube (PET, Graßmann and Peters, 2002). When comparing the pressure dependent measurements of n-propanol with measurements of n-butanol (Hyvärinen et al., 2006, 2008) and n-pentanol (Brus et al., 2008; Anisimov et al., 2000), a positive pressure effect is observed in all of these measurements, which is more pronounced at lower temperatures. The pressure effect is smaller for propanol than butanol and pentanol. The results found here confirm the expectations (Hyvärinen et al., 2006, 2008; Brus et al., 2008) that the pressure effect is more pronounced for n-alcohols with longer carbon chain length.

3.2.2 Homogeneous binary nucleation of H_2SO_4-H_2O

A laminar flow tube was used for the H_2SO_4-H_2O nucleation experiment, with the furnace as a source of sulphuric acid vapour to compare atmospheric and experimental data (**Paper III**). Formation rates were observed at three different nucleation temperatures (278 K, 288 K and 298 K) and at three different levels of relative humidity (16 %, 32 %, and 57 %). Particle concentration was measured with PSM and the gas phase sulphuric acid with CIMS. The wall losses in the flow tube and measurement system were determined to be able to calculate the initial concentration when the actual nucleation took place. These results were compared to atmospheric data analysed by Paasonen et al. (2010) from three sites (Hyytiälä, Finland; Melpitz, Germany; San Pietro Capofiume, Italy), where the formation rates of 2 nm particles (J_2) were closely connected to the gas phase sulphuric acid concentration measured with CIMS. This type of dataset is directly comparable to the data measured in **paper III**, where PSM and CIMS were used.

The data comparison is presented in Fig. 6. It is evident from the figure that most of the experimental data obtained in this study are in good agreement with the atmospheric data. However, the data with the lowest RH (16 %) and the highest temperature (298 K) do not fit the atmospheric data. Paasonen et al. (2010) reported the median kinetic and activation coefficient (table 4 in Paasonen et al., 2010) to be $K = 26 \times 10^{-14}$ cm^3 s^{-1} and $A = 9.7 \times 10^{-7}$ s^{-1}, whereas in this study the median coefficients were found to be $K = 0.1 \times 10^{-14}$ cm^3 s^{-1} and $A = 7.85 \times 10^{-7}$ s^{-1}. The exponents E were determined from the linear fits to the experimental data from 1.2 to 2.2, depending on the relative humidity and temperature. Even though the coefficients are similar between the laboratory and atmospheric measurements, one must use caution when interpreting this, as the coefficients may depend on other quantities, such as the concentration of organic vapours (Paasonen et al., 2010).

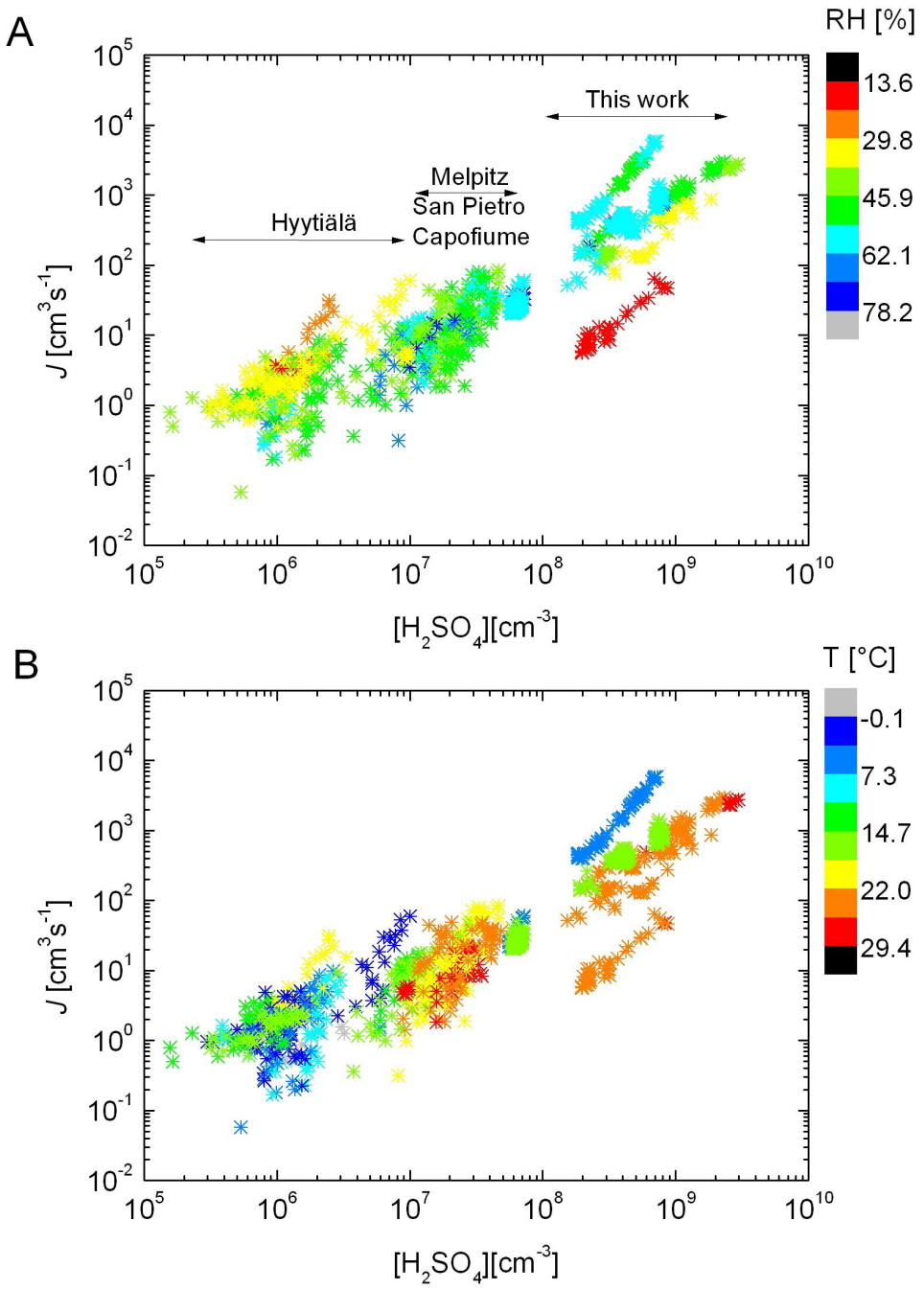

Figure 6. Nucleation rates as a function of sulphuric acid concentration, comparison of atmospheric data (Paasonen et al., 2010) and results from **Paper III** according to relative humidity (A) and temperature (B). Figure adapted from **Paper III**.

3.2.3 Homogeneous ternary nucleation of H_2SO_4-H_2O-base

According to Kashchiev (1982) the relationship between nucleation rates and nucleating vapour concentration can de deduced from the number of molecules within the critical cluster (for sulphuric acid case, $d\ln J / d[H_2SO_4]$), which is the slope of each data set presented in Fig 6. For atmospheric and laboratory studies the slope has been found to be between 1 and 2, but according to CNT the slope should be between 4 and 9. As a solution to this problem, it has been suggested that other species like ammonia and amines (Weber et al., 1996; Berndt et al., 2010) or organic acids (Zhang et al., 2004; Zhang, 2010; Metzger et al., 2010; Paasonen et al., 2010) have a stabilizing effect on the sulphuric acid containing clusters, reducing the necessary concentration of sulphuric acid for nucleation. Recent laboratory studies have indeed shown large enhancement of nucleation rates when introducing amines or ammonia into the H_2SO_4-H_2O system (Ball et al. 1999, Benson et al. 2009, Berndt et al. 2010, Erupe et al. 2010, Benson et al. 2011, Kirkby et al. 2011, Zollner et al. 2012 Almeida et al. 2013).

To study the effect of four base species (ammonia, monomethyl amine (MMA), dimethyl amine (DMA) and trimethylamine (TMA)) on H_2SO_4-H_2O nucleation, we applied the laminar flow tube with the saturator as a source of sulphuric-acid vapour (**Paper IV**). The gas-phase base compounds were produced from a permeation tube placed inside a constant temperature oven (313 K). The base compound evaporates from the tube into a carrier gas flow, which is further cleaned with scrubbers in the calibration unit before entering the oven. Two separate experiments were done. In the first experiment, sulphuric acid concentration was measured with CIMS and the base compound input was determined. In the second, sulphuric acid input was determined and the base concentration was measured with MARGA. The procedure was the same in both experiments: First, H_2SO_4-H_2O nucleation rates were measured to ensure the reproducibility of the data and second, the base compound was introduced starting from approximately 30 pptv, increasing the concentration in a stepwise manner every 6–12 hours, up to several thousands of pptv. The sulphuric-acid concentration was kept constant throughout the experiments.

Only TMA was found to enhance nucleation in this work, with a maximum enhancement factor of 5.5 at TMA concentration of 2500 pptv, where the enhancement effect was saturated. Other compounds did not enhance the nucleation rate and it is thought that the trace levels of these compounds in the carrier gas and from the ultra-pure water used for humidification were enough to already saturate the effect. The concentration of amines and ammonia, where the enhancement was found to saturate in the studies listed in Table 1, are well below the MARGA detected background concentration (ammonia, 201 pptv) and are below the detection limits of MARGA (72, 149 and 294 pptv for MMA, DMA and TMA, respectively), which supports the assumption of saturation by background trace levels. The various saturation levels and enhancements in Table 1 are due to a wide range of conditions, such as temperature, RH and sulphuric acid concentration.

Table 1. Collected information from several studies found in the literature on base substances enhancing sulphuric acid-water nucleation. The enhancement factors are not always

the highest found in those studies, but are the maximum enhancement with the closest conditions to the conditions used in this study. Listed are the base substance used, relative humidity (RH), nucleation temperature (T_{nucl}), sulphuric acid concentration [H_2SO_4], base concentration [base], enhancement factor (EF) and the carrier gas used. *Almeida *et al*. (2013) carried out their experiment in two parts; in the first part 0.1–5 pptv of DMA was introduced to the system resulting in an EF of 10^6. Increasing the DMA concentration resulted into an EF of 100 more, but they did not report any saturation of the effect. Table adapted from **Paper IV**.

Study	***Substance***	***RH (%)***	***T_{nucl} (K)***	***[H_2SO_4] (cm^{-3})***	***[base] (pptv)***	***EF***	***Carrier gas***
Ball et al. (1999)	NH_3	15	295	$3\ 10^9$	80	10	N_2
Berndt et al. (2010)	NH_3	41	293	10^7	44635	5	Synth. air
Benson et al. (2011)	NH_3	13-16	288	$5\ 10^6$	1220	1-1.5	N_2
Kirkby et al. (2011)	NH_3	38	292	$1.5\ 10^8$	100	10^2	Synth. air
Zollner et al. (2012)	NH_3	27	296	$3\ 10^9$	45	$1.4{\cdot}10^5$	N_2
Zollner et al. (2012)	MMA	27	296	$3\ 10^9$	35	$2.\ {\cdot}10^6$	N_2
Almeida et al. (2013)	DMA	38	278	10^7	0.1-5*	10^6	Synth. air
Almeida et al. (2013)	DMA	38	278	$2\ 10^6$	13-140*	10^2	Synth. air
Erupe et al. (2011)	TMA	25	288	10^7	1350	8	N_2
This study	TMA	30	298	$2.8\ 10^6$	2500	5.5	air

3.3 Sulphuric-acid monomer vs. total sulphate in nucleation studies

Laboratory experiments on sulphuric-acid nucleation has been conducted since early 1990s, with a variety of sulphuric-acid production and detection methods, as well as results (e.g. Wyslouzil et al., 1991; Viisanen et al., 1997; Brus et al., 2010; Zollner et al., 2012). In the earlier experiments the sulphuric acid concentration was determined as relative acidity (Wyslouzil et al., 1991) from the saturation vapour pressure of sulphuric acid. Later, when direct measurements of gas phase sulphuric acid became possible through the introduction of CIMS, similar nucleation rates were produced with several orders of magnitude smaller sulphuric acid concentrations (e.g. Young, et al., 2008) than had been determined from the vapour pressure.

A similar discrepancy in sulphuric-acid concentration was observed in **Paper III**, where the mass-balance calculation for the input of sulphuric acid from the furnace into the flow tube was approximately 2 orders of magnitude higher than the CIMS measured concentration at the end of the flow tube. After careful measurements and determination of the wall loss factor (WLF) in the flow tube and wall loss factor of the CIMS inlet (WLF_{inlet}), the measured gas-phase sulphuric-acid concentration was converted to the initial value at the beginning of the flow tube, but the initial concentration was still approximately one-to-two orders of magnitude lower than calculated from the mass balance. The discrepancy may arise from some trace species reacting with sulphuric acid molecules, thus preventing them from detection by mass spectrometers. The discrepancy was the motivation for **Paper V** and the possible reasons for the discrepancy are discussed in chapter 3.3.1.

To find out the reason for this discrepancy, rigorous tests with a saturator (Fig. 3) were done with two independent methods of detecting sulphuric acid (mass spectrometry and ion chromatography). After the tests, the saturator was used in combination with the laminar flow tube for the H_2SO_4-H_2O binary nucleation experiment so as to enable a comparison with the experiment where the furnace was used as the source of the sulphuric acid vapour (**Paper III**; Brus et al, 2010). With this comparison it was possible to rule out the sulphuric-acid-vapour production method as the reason for the discrepancy in the observed sulphuric-acid concentration.

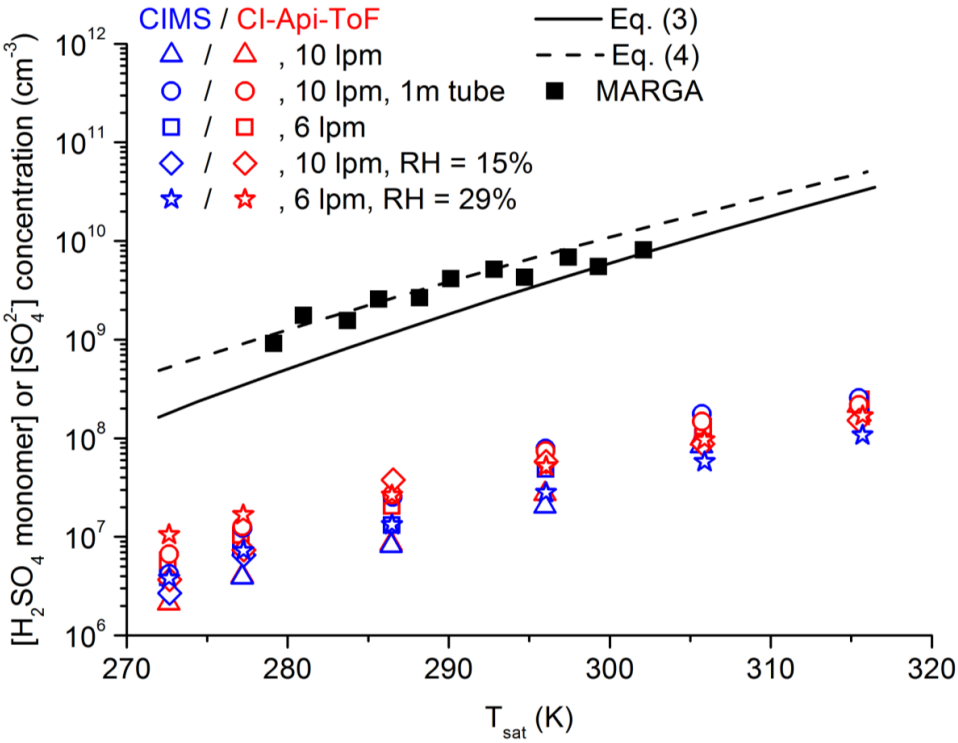

Figure 7. Measured sulphuric-acid monomer [H_2SO_4 monomer] and total-sulphate [SO_4^{2-}] (black squares) concentrations together with predicted values by Eq. (3) and (4) as a function of saturator temperature T_{sat}. The saturator flow rate is Q_{sat} = 0.5 lpm and mixing flow rates were 40 lpm (dry for CIMS and CI-APi-TOF and RH 15 %) and 20 lpm (MARGA and RH 29 %). CIMS (blue markers) and CI-APi-TOF (red markers) have been tested with 6 lpm and 10 lpm (nominal) inlet total flow rates and also with an extra 1 m Teflon tubing after the saturator. Figure adapted from **Paper V**.

The saturator tests with mass spectrometers (CIMS and CI-APi-TOF) were done with two inlet flow rates (nominal 10 lpm and 6 lpm), in dry (RH of 0 %) and humid conditions (RH of 29 and 15 % for 6 and 10 lpm inlet flow rates, respectively) and with an extra 1 m line between the outlet of the saturator and the mixer, where the dilution flow (20 lpm for RH of 0 and 15 %, 40 lpm for RH of 29 %) was mixed with the flow from the saturator (0.5 lpm). These tests were done to check if changing the inlet flow rate would change the calibration factor, to test if hydration of the sulphuric acid clusters due to the high hygroscopicity would alter the measured concentration, and to test the effect of wall losses. The tests with an ion chromatograph (MARGA) were conducted only in dry conditions, as the conditions inside MARGA are supersaturated with water vapour, suggesting that initial RH should not affect the measured sulphate concentrations. The obtained results were compared to the theoretical predictions from vapour pressure (Eqs. 3 and 4) as well as to each other (Fig. 7). As seen in Fig. 7, MARGA-measured total-sulphate concentration agrees very well with the prediction

of Eq. (4), while CIMS and CI-APi-TOF measured sulphuric-acid-monomer concentration is one-to-two orders of magnitude lower. Relative humidity, inlet flow rate, or the extra 1 m tube affects the measured sulphuric-acid-monomer concentration very little. Larger clusters containing solely sulphuric acid were left out of the analysis as the concentration of dimers was always in the range of 1 % of the monomers, while the trimers were in the range of 1 % of the dimers, continuing with a similar ratio towards larger clusters, which supports earlier findings (Jokinen et al., 2012).

To investigate the discrepancy further, the saturator was applied as a source of sulphuric-acid vapour for the H_2SO_4-H_2O nucleation experiment to enable a comparison with the results obtained with the furnace as the source of sulphuric acid. The sulphuric-acid or total-sulphate concentrations were measured with CIMS (**Paper III**) and bubblers (Brus et al., 2010) with the furnace as part of the system. The comparison of the apparent formation rates J as a function of the measured sulphuric-acid-monomer or total-sulphate concentration is presented in Fig. 8. The conditions were similar (T = 298 K, RH ~30 %) in all experiments excluding the residence time, which was defined differently in the experiments with the furnace (Brus et al., 2010; Herrmann et al., 2010). Due to the different definition of the residence time, the formation rates have a factor of two difference. Nevertheless, the data sets in Fig. 8 agree very well, when considering different sulphuric-acid-detection methods separately. The discrepancy of the measured sulphuric-acid or total sulphate concentrations with similar formation rates and conditions from the same flow tube persists.

As MARGA and bubblers trap all sulphate (i.e. in the gas and particle phase), the maximum amount of sulphuric acid in the particles was determined by measuring the particle number size distribution at the end of the flow tube and assuming they consisted of pure sulphuric acid. The maximum amount of sulphuric acid in the particle phase was found to range from 0 to 1.4 % of the total sulphate concentration. Total Loss Factors (TLFs) were determined by measuring the concentration from the saturator only and subtracting the concentration measured at the end of the flow tube for both instruments separately. TLFs contain the losses to the walls and the losses to the particles due to nucleation and growth. The average values of TLFs were 14.2 ± 4.2 for CIMS and 10.0 ± 1.2 for MARGA. The discrepancy could not be explained with the losses in the flow tube or to the particle phase.

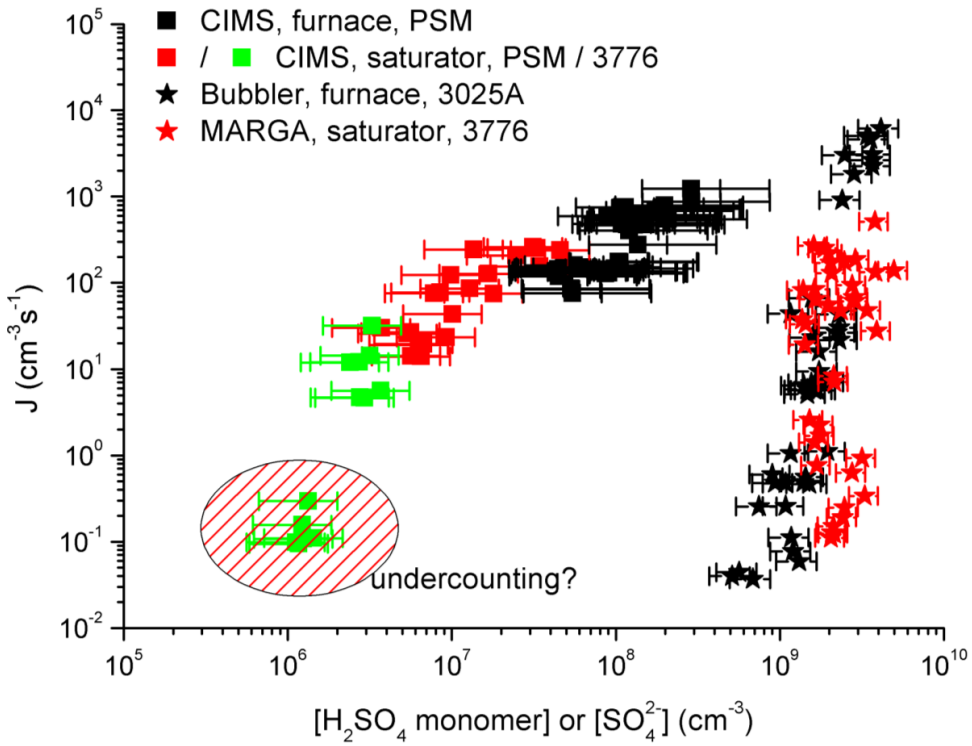

Figure 8. Comparison of formation rates *J* as a function of residual sulphuric-acid-monomer concentration [H_2SO_4] or total-sulphate concentration [SO_4^{2-}] to our previous results. Conditions are similar (T =298 K, RH ~30 %). Note the factor-of-two difference between the residence times between the furnace and saturator measurements. Sulphuric-acid vapour was previously produced with the furnace method and total-sulphate concentration measured with the bubbler method (Brus et al., 2010). Figure adapted from **Paper V**.

3.3.1 Distribution of sulphuric acid to clusters and early growth of particles due to total sulphate

As stated in the literature (e.g. Benson et al., 2011; Kirkby et al., 2011) contaminants are present in almost every laboratory experiment. These contaminants may bond with the sulphuric acid molecules, and in some cases prevent them from charging in the CI-inlet and hence, being detected by the mass spectrometers. To ensure that the contaminant levels in the carrier gas (pressurized, purified air) were sufficiently low, the saturator tests were extended to three different purity carrier gases (N_2 6.0, N_2 5.0 from a cylinder and liquid source, pressurized air). Also, two different purities of sulphuric acid were used (100 % and 97 %) as the liquid sulphuric acid inside the saturator. The sulphuric-acid concentration was measured with CI-APi-TOF to observe if different contaminant levels would change the cluster distribution of pure sulphuric acid clusters (monomers, dimers and trimers). The measured cluster concentrations with different carrier gases as a function of the saturator

flow rate with a constant saturator temperature (288 K) are presented in Fig 9. The theoretical prediction from vapour pressure (Eq. 3) is also plotted for comparison. The first test was done with the purest gas (N_2, 6.0) after cleaning the setup (Fig. 3). Due to the cleaning, the walls of the system were not saturated with sulphuric acid, resulting in lower concentration than expected for the first two points (two lowest saturator temperatures for N_2, 6.0). It is evident from the figure that the cluster distribution is independent of the carrier gas, confirming that the carrier gas used in this study was at least as clean as the purest commercially available gas and proving the suitability of the choice for the carrier gas. The purest commercially available carrier gas (N_2, 6.0) has impurities of less than 0.5 ppm of H_2O and O_2 and less than 0.1 of hydrocarbons (C_nH_m). The monomer concentration is one-to-two orders of magnitude lower than the prediction by Eq. (3), as previously. Several different tests were done as a function of the saturator temperature and saturator flow rate, all resulting to the same conclusion, that the carrier gas was sufficiently pure.

The measurements with different carrier gases were further investigated to establish the fate of the "lost" sulphuric acid. The CI-APi-TOF mass spectra were averaged over time the system was in a steady state (i.e. constant monomer concentration) for each carrier gas and the signals were averaged to the nearest unit mass-to-charge (i.e. unit-mass-resolution, UMR-sticks). The signals below 500 Th were correlated to a mass of 97 Th (HSO_4^-), which is the ionized sulphuric acid monomer (Fig. 10). The number of correlating (and anti-correlating) peaks increases as a function of the increasing saturator temperature with all three carrier gases (N_2, 5.0 showed in Fig. 10) and the number of these peaks are similar with all carrier gases at similar temperatures. The correlating peak's (*m/Q*)-position differs between carrier gases, suggesting different contaminants in the carrier gases. Figure 10 show that the sulphuric acid is distributed to a wide range of cluster configurations, which are not used in calculation of the monomer, dimer or trimer concentrations, i.e. not detected as sulphuric acid when measured with mass spectrometers. Unfortunately calculating the actual concentration of the sulphuric acid in these clusters is impossible, as their charging efficiency (i.e. calibration constant) and their chemical composition are unknown. This prevents summing the total sulphuric acid concentration even from the peaks that correlate with 97 Th. The peaks in Fig. 10 are only those below 500 Th and showing relatively large (anti-) correlation with the HSO_4^-, but the actual mass spectrum of CI-APi-TOF contains an even-larger amount of signal peaks, as not all the peaks (anti-) correlate with a peak of 97 Th. The mass spectra were zoomed further and the number of peaks increases rapidly. The peaks that are averaged in to one UMR-stick, could be separated by a high resolution (HR-sticks) analysis (Junninen, 2013) but going through all of the correlating peaks is a very demanding task and is beyond the scope of this work.

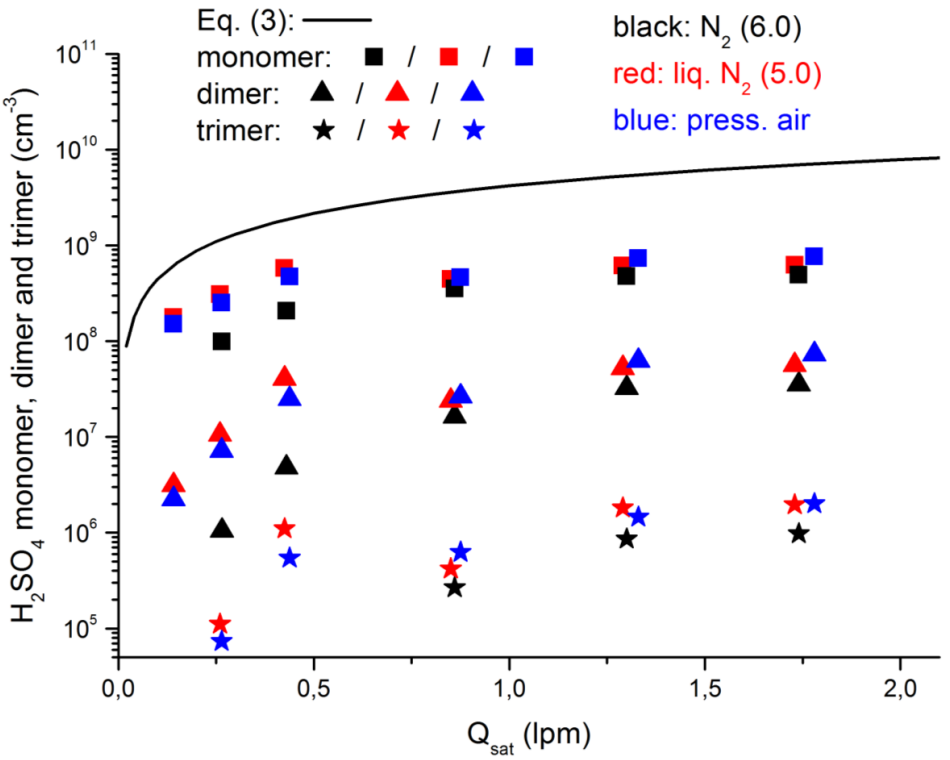

Figure 9. CI-APi-TOF measured H_2SO_4 monomer, dimer and trimer concentrations as a function of saturator flow rate Q_{sat}, with three different carrier gases compared to the prediction from Eq. (3) at a saturator temperature of 288 K. The two points at the lowest saturator temperature measured using N_2 (6.0) are lower than expected due to cleaned measurement lines, where the walls were not yet saturated. The y-axis is limited to $5 \cdot 10^4$ cm^{-3} which is considered to be the lower detection limit of the CI-APi-TOF.

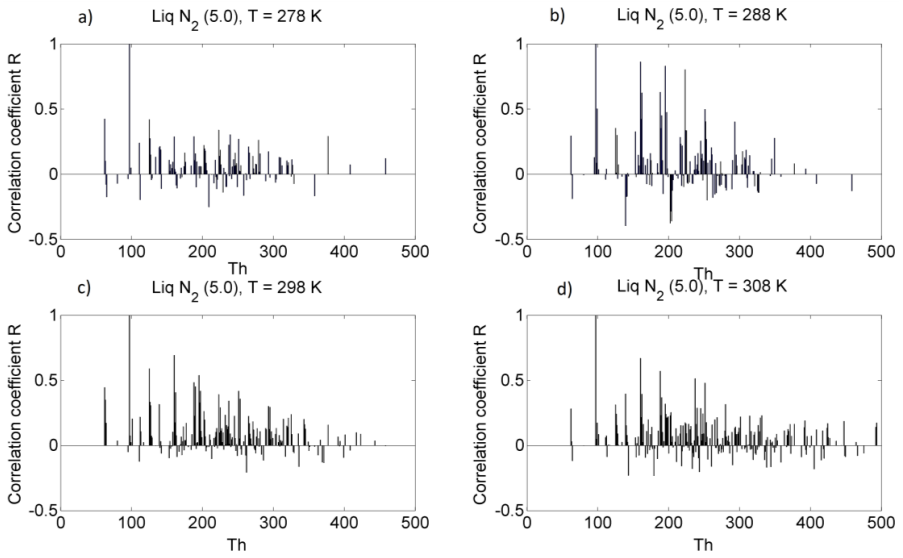

Figure 10. Correlation coefficient of stick masses below 500 Th to 97 Th (HSO_4^-) at four different saturator temperatures (278 K, 288 K, 298 K and 308 K) with N_2 (5.0) from liquid source as a carrier gas. Figure adapted from **Paper V**, Supplementary material.

The model from Škrabalová et al. (2014) was used to calculate the resulting particle diameter (D_p) and growth rates (GR) of the particles, using the measured sulphuric-acid-monomer and total-sulphate concentration observed in the nucleation experiments with the flow tube. The measured concentrations were converted to the initial value with the use of Total Loss Factors (TLFs, chapter 3.3). The initial size of the clusters was chosen to be 1.5 nm (Kulmala et al., 2007). The residence time was 30 s. The model uses three different ammonia uptake scenarios: (0) no uptake of ammonia, particles composed of sulphuric acid and water, (1) uptake of ammonia at the same rate as sulphuric acid, resulting in ammonium bisulphate-water particles and (2) double uptake rate of ammonia compared to sulphuric acid, forming ammonium sulphate-water particles.

With the initial sulphuric-acid monomer as an input parameter, the growth rates ranged approximately from 1 to 15 nm h^{-1} as a function of sulphuric-acid concentration (i.e. saturator temperature T_{sat}). With these growth rates, the resulting diameters were below 2 nm, which are drastically smaller than the observed mean diameters (Fig. 11, upper panel). When using initial total-sulphate as an input, the growth rates were much larger, ranging from 1250 to 2300 nm h^{-1}, depending on the model scenarios (0, 1 or 2) used and the total-sulphate available. Using these growth rates, the resulting particle diameters were similar to the observed mean diameters (Fig. 11, lower panel). The initial growth after nucleation might be dominated by sulphate, instead of the marginal growth calculated from the mass-spectrometer-measured sulphuric acid, explaining the high growth rates in the flow tube, compared to the typical values measured in the atmosphere.

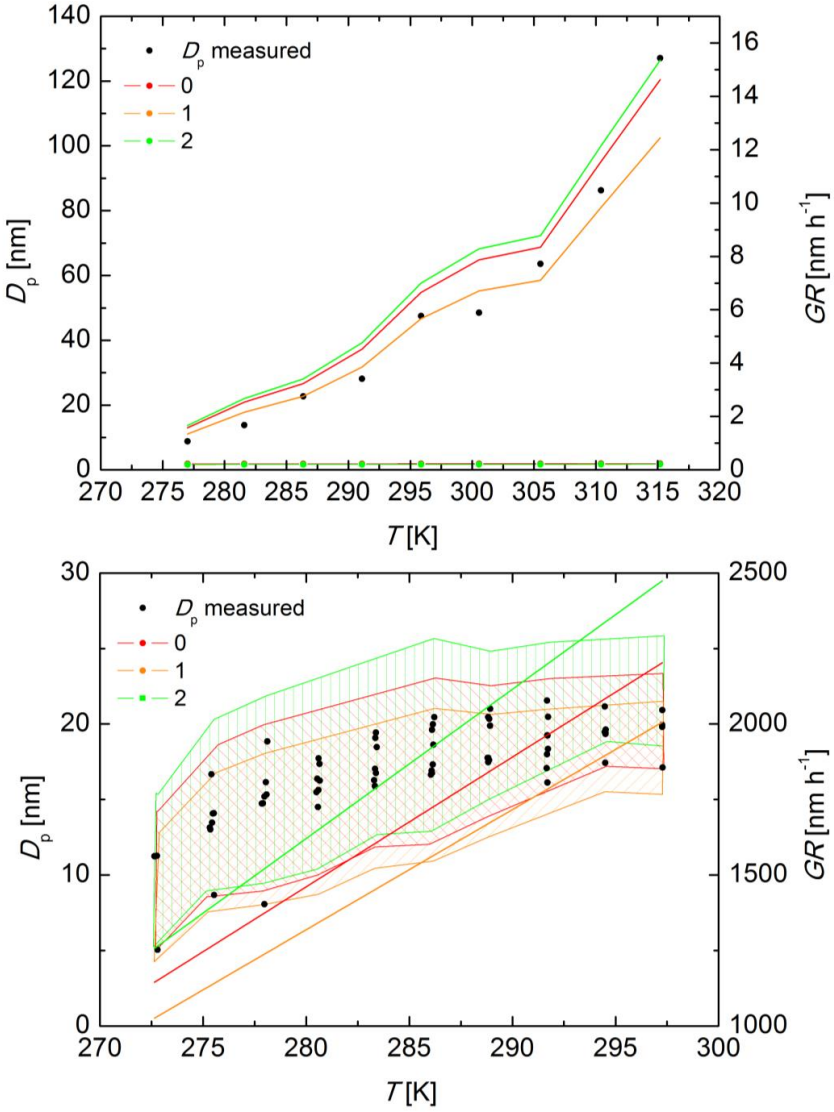

Figure 11. Modelled particle diameters D_p and growth rates GR as a function of the saturator temperature T_{sat} using 1.5 nm as an initial cluster size and initial sulphuric-acid-monomer (left panel) or initial total-sulphate concentration (lower panel) as an input for the model. Solid lines are growth rates, lines with symbols (upper panel) or shaded area (lower panel) are the modelled diameters and black dots are measured geometric mean diameters. Three different ammonia uptake scenarios are used: (0) no uptake of ammonia, (1) uptake of ammonia with the same rate as sulphuric acid and (2) double uptake rate for ammonia, compared to sulphuric acid. Shaded area on the panel on the right is between the minimum and the maximum modelled particle diameter, using minimum and maximum measured total-sulphate concentration on the same saturator temperature. Figure adapted from **Paper V**, Supplementary material.

4 Review of the papers and authors contribution

Papers in this thesis consider data evaluation of atmospheric new particle formation from the field and laboratory studies on unary, binary and ternary homogeneous nucleation.

Paper I presents a data evaluation of new particle formation (NPF) in the foothills of the Himalayas. The NPF events were classified and the characteristics of the event were determined. The NPF events were found to be sparse and very seasonal. The seasonality was explained by the planetary boundary layer (PBL) evolution, due to the increased solar radiation during spring, increasing the maximum PBL height above the station and bringing nucleation precursor gases and the nucleated particles to the station. In this paper I was responsible for most of the writing and the data analysis.

Paper II describes the measurements and data evaluation of isothermal unary homogeneous nucleation of n-propanol in helium in a laminar flow diffusion chamber (LFDC) and especially the pressure effect of the carrier gas on the observed nucleation rates. The nucleation rates were compared to n-propanol nucleation rates measured with other instruments found in the literature and to theoretical predictions using classical nucleation theory (CNT). The observed nucleation rates agree with the experimental literature values and with the CNT prediction. A small positive pressure effect was observed, which fits well within the homologous series of n-alcohols. The suggestion that the effect is less pronounced for alcohols with shorter carbon chain length is confirmed. Comparison of the pressure effect to the theoretical approach by Wedekind et al. (2008) agrees in the main, but the degree of the effect is much larger than expected by the theory. I participated in most of the measurements and data evaluation on this paper and wrote part of the manuscript.

Paper III reports results on binary homogeneous nucleation of sulphuric acid and water, which was conducted using a laminar flow tube and furnace as a source of the sulphuric acid vapour. The formation rates were measured at three different relative humidities and at three different temperatures. The wall losses in the flow tube were experimentally determined. The experimental formation rates as a function of gas-phase sulphuric acid were compared to atmospheric data from three different sites in Europe at different temperatures and different relative humidities. Laboratory results agreed very well with the atmospheric data, with a slight underestimation by the laboratory data at the lowest relative humidity and the highest temperature. The empirically determined coefficients for kinetic- and activation-model nucleation were similar to those determined from the atmospheric data. The exponential dependence of the formation rate on the sulphuric-acid concentration was found with the exponent between 1.2 and 2.2, which is typical for the atmospheric data. I participated in all of the measurements in this paper and performed most of the data analysis.

Paper IV studies the ternary homogeneous nucleation of sulphuric acid, water and four base compounds (ammonia, monomethyl amine, dimethyl amine and trimethyl amine), separately. The same flow tube was used in this work as previously but a saturator was used as a source of sulphuric-acid vapour. The enhancement of the observed H_2SO_4-H_2O formation rates by adding a base compound was studied and compared to similar experiments found

in the literature. An enhancement factor of 5.5 was observed with trimethyl amine at a concentration of 2500 pptv. No enhancement with other base compounds was observed, suggesting that the effect was already saturated due to the contaminants in the carrier gas and water used for the humidification. Measured concentrations of the contaminants were below detection limits for amines, while the background concentration of ammonia was found to be 201 pptv. The detection limits provided the maximum limit of the contaminants and a comparison to the literature provided an estimate of the levels of these compounds, where the enhancement is saturated. I planned and conducted most of the measurements in this paper, as well as wrote most of the paper.

Paper V studies the observed discrepancy of one-to-two orders of magnitude between measured sulphuric-acid-monomer (mass spectrometers) and total-sulphate (ion chromatographs) concentrations. A saturator was used as a source of sulphuric-acid vapour and it was tested with the two independent sulphuric-acid-detection methods. A H_2SO_4-H_2O nucleation experiment was conducted to enable a comparison with the previous results, where a furnace was used as the source of the sulphuric acid. The saturator was tested with three different levels of purity for the carrier gases (N_2, 6.0 and 5.0 and pressurized, purified air) to ensure sufficient purity of the carrier gas. The mass spectra of the high resolution mass spectrometer were further analysed to find the reason for the discrepancy. A model was used to calculate growth rates and resulting diameters and compared to the experimental diameters. The production method of the sulphuric-acid vapour was found to be indifferent, ruling it out as the reason for the discrepancy. Wall losses and losses to the particle phase were determined to be minor. Tests with different purity carrier gases proved to produce similar sulphuric-acid concentrations and cluster distributions. A deeper analysis of the mass spectra revealed that the sulphuric acid is distributed into a wide range of clusters, which is not taken into account when calculating the sulphuric-acid monomer, dimer or trimer concentration. The number of these sulphuric-acid-containing peaks suggests a vast number of clusters which might function as a start for atmospheric nucleation. The model suggests that the initial growth of the freshly formed particles can be dominated by sulphate. In this paper, I made most of the measurements and data evaluation, as well as wrote the paper.

5 Conclusions

In the work presented in this thesis, atmospheric nucleation was approached experimentally from two different points of views, with field measurements and with laboratory experiments. From a four-year dataset obtained in the foothills of the Himalayas, the new particle formation (NPF) events were classified and the characteristics of the events were analyzed (**Paper I**). The meteorological conditions and the vertical extent of the events were determined. The laboratory experiments presented in this work have given an insight into the carrier gas pressure effect observed in unary homogeneous nucleation of n-alcohols, extending the already available literature data (**Paper II**). The importance of these types of data is in the testing of different theories (for example, classical nucleation theory, CNT), which are not able to sufficiently predict even the simplest experimentally determined nucleation rates. The laboratory experiments for binary or ternary nucleation (**Papers III-IV**) provided an insight into the sulphuric-acid-concentration dependence of particle formation rates at close to atmospheric conditions at different temperatures, as well as information on the important role of base compounds in atmospheric nucleation and at what concentrations. An observation of a large discrepancy between the measured sulphuric-acid monomer and total-sulphate concentrations from the same sulphuric acid source led to an investigation of the distribution of sulphuric acid into clusters, and modelling of the early growth of sulphate or sulphuric-acid monomer (**Paper V**). The work in **Paper V** provided an insight into numerous clusters that might act as a starting point for atmospheric nucleation and the early growth of freshly nucleated particles. This work also provided deeper information about contaminants in laboratory nucleation studies.

This thesis has contributed to the understanding of atmospheric nucleation in the following way, achieving the three main goals set out in the introduction:

1. Characterize the new particle formation event in the foothills of the Himalayas

The NPF events were classified and analyzed. The NPF events were found to be relatively sparse, with extremely high seasonality with maximum during spring months. The seasonality was explained with the meteorological conditions, especially the height of the planetary boundary layer (PBL). During spring months the modelled PBL maximum height reached the altitude of the station, providing precursor gases from lower altitudes and diluting the Condensational Sink (CS), which made the conditions favourable for nucleation. The NPF events were nearly always occurring in the boundary layer, except for the sporadic NPF event observed outside spring months, which can be considered as free tropospheric formation events.

2. To gain insight into unary, binary and ternary nucleation mechanisms by means of laboratory experiments

Isothermal nucleation rates of propanol in helium were measured using a laminar flow diffusion chamber (LFDC) at different temperatures and carrier gas pressures. The results were compared to literature values as well as to theoretical predictions. A small positive pressure

effect on the nucleation rate was observed, which strengthens the assumption that this effect depends on the carbon chain length of the n-alcohols, reducing as a function of increasing chain length. Comparison to the theoretical approach of Wedekind et al. (2008) showed a similar trend in the pressure effect, though the experimental results produced a stronger effect.

Binary nucleation rates of H_2SO_4-H_2O were measured using a laminar flow tube in close-to-atmospheric conditions at different temperatures and relative humidities. The experimental results were analyzed to obtain empirical coefficients for activation and kinetic parameterizations, which were compared to atmospheric data from three different sites in Europe. The formation rates as a function of sulphuric-acid concentration agreed well with the atmospheric data, except for the highest temperature and lowest relative humidity. The obtained coefficients were in fairly good agreement with the atmospheric data. The formation rate was determined to depend on the sulphuric acid concentration with an exponent between 1.2 and 2.2. A large range of power dependencies are reported in the literature. For example Zollner et al. (2012) reported power dependencies in the range of 4.5–7 for their laboratory experiments. Sipilä et al. (2010) report power dependencies of 1.0–2.1 for their laboratory studies, showing similar results to our study. Results reported from the atmospheric measurements (Kuang et al., 2008; Paasonen et al., 2010) agree with this study.

Ternary nucleation rates of H_2SO_4-H_2O-base were measured with four different base substances (ammonia, monomethyl amine, dimethyl amine and trimethyl amine) separately and the obtained results were compared to other similar studies found in the literature. Only trimethyl amine was found to enhance nucleation, as the effect of other base compounds used was already saturated by the contaminants in the carrier gas or from the water used for humidification. The measured background concentrations of the amines were below detection limits, providing the maximum limit for the background concentration. A comparison with the literature values reinforced the assumption that the enhancement was already saturated below the detection limit of the instrument used.

3. To establish the reason behind the discrepancy between measured total-sulphate and sulphuric-acid monomer concentrations with two independent sulphuric-acid-detection methods, and to study the implication of the discrepancy on early growth of freshly formed particles

The observed discrepancy was characterized with rigorous testing with a saturator and two independent methods to detect sulphuric acid. The saturator was used also in combination with a laminar flow tube in a nucleation experiment to enable a comparison with earlier results, where a furnace was used, to rule out the sulphuric-acid-vapour-production method as a reason for the discrepancy. The tests included three different purities of carrier gases (N_2 6.0, N_2 5.0 from liquid and gas source and purified, pressurized air) and two purities of sulphuric acid (97 and 100 %). The measured total-sulphate concentrations agreed well with theoretical predictions from vapour pressure, as the measured sulphuric-acid-monomer concentrations were one-to-two orders of magnitude lower. Similar results were found in earlier results where a furnace was used, ruling out the sulphuric acid vapour production method

as the reason for the discrepancy. Analysis of the nucleation experiment with the laminar flow tube proved that the "lost" sulphuric acid is not in a particle phase, nor is it lost to the walls of the flow tube. Larger clusters containing solely sulphuric acid (dimer, trimer, etc.) were also shown to be ineffective in explaining the discrepancy.

Tests with different purity carrier gases showed that the purified, pressurized air used in the nucleation experiment was as clean as the purest commercially available gas. Further analysis of the mass spectra from CI-APi-TOF provided insight into the cluster distribution with different carrier gases. The number of peaks correlating with a mass of 97 Th (HSO_4^-, ionized sulphuric acid monomer) was very large and it increased as a function of sulphuric-acid concentration, suggesting very large concentrations of sulphuric-acid-containing clusters, which are not used when calculating the sulphuric-acid concentration from mass spectrometer data. These clusters can act as a beginning for atmospheric nucleation. The discrepancy is due to the different contaminant species binding sulphuric-acid monomers from the free gas-phase form into clusters that are not taken into account in the calculation of gas-phase sulphuric acid concentration.

The measured total-sulphate and sulphuric-acid concentrations were used as input parameters for a model to calculate growth rates and resulting diameters for the nucleation experiment with the flow tube, with the modelled results compared to the experimentally obtained ones. The comparison showed that the sulphuric-acid monomer is not able to produce the experimentally observed diameters, but the total sulphate was able to. According to the model, sulphuric acid may be responsible for a much larger fraction of the initial growth of the freshly nucleated particles than would be calculated from the mass spectrometer measured monomer, dimer and trimer concentrations. Nevertheless, the sources of sulphate are much more numerous than merely from sulphuric acid and there are numerous compounds that possibly contribute to the growth of the particles in the atmosphere. More detailed measurements are needed on particles' chemical composition throughout the particle growth, from nucleated clusters to larger particles, and to establish the contribution of sulphate in the particle growth.

References

Agarwal, J. K. and G. J. Sem (1980). Continuous flow, single-particle-counting condensation nucleus counter. J Aerosol Sci., 11, 4, 343-357.

Aitken, J. (1888). On the number of dust particles in the atmosphere. Trans. Roy. Soc., Edinburgh, 35, 1-19.

Almeida, J., S. Schobesberger, A. Kürten, I. K. Ortega, O. Kupiainen-Määttä, A. P. Praplan, A. Adamov, A. Amorim, F. Bianchi, M. Breitenlechner, A. David, J. Dommen, N. M. Donahue, A. Downard, E. Dunne, J. Duplissy, S. Ehrhart, R. C. Flagan, A. Franchin, R. Guida, J. Hakala, A. Hansel, M. Heinritzi, H. Henschel, T. Jokinen, H. Junninen, M. Kajos, J. Kangasluoma, H. Keskinen, A. Kupc, T. Kurtén, A. N. Kvashin, A. Laaksonen, K. Lehtipalo, M. Leiminger, J. Leppä, V. Loukonen, V. Makhmutov, S. Mathot, M. J. McGrath, T. Nieminen, T. Olenius, A. Onnela, T. Petäjä, F. Riccobono, I. Riipinen, M. Rissanen, L. Rondo, T. Ruuskanen, F. D. Santos, N. Sarnela, S. Schallhart, R. Schnitzhofer, J. H. Seinfeld, M. Simon, M. Sipilä, Y. Stozhkov, F. Stratmann, A. Tomé, J. Tröstl, G. Tsagkogeorgas, P. Vaattovaara, Y. Viisanen, A. Virtanen, A. Vrtala, P.E. Wagner, E. Weingartner, H. Wex, C. Williamson, D. Wimmer, P. Ye, T. Yli-Juuti, K. S. Carslaw, M. Kulmala, J. Curtius, U. Baltensperger, D. R. Worsnop, H. Vehkamäki and J. Kirkby (2013). Molecular understanding of sulphuric acid–amine particle nucleation in the atmosphere. Nature, 502, 359-363, doi: 10.1038/nature12663.

Anisimov, M. P., P. K. Hopke, S. D. Shandakov and I. I. Shvets (2000). n-pentanol–helium homogeneous nucleation rates J. Chem. Phys. 113, 1971–1975, doi: 10.1063/1.482002.

Apte J., T. Kirchstetter, A. Reich, S. Deshpande, G. Kaushik, A. Chel, J. Marshall and W. Nazaroff (2011). Concentrations of fine, ultrafine, and black carbon particles in auto-rickshaws in New Delhi, India. Atmos. Env., 45, 4470-4480, doi:10.1016/j.atmosenv.2011.05.028.

Arnold, F. (1980). Ion-induced nucleation of atmospheric water vapor at the mesopause. Planetary and Space Science, 28, 10, 1003-1009, doi: 10.1016/0032-0633(80)90061-6.

Ayers, G. P., R. W. Gillett and J. L. Gras (1980). On the vapor pressure of sulphuric acid. Geophys. Res. Lett., 7, 6, 433-436, doi: 10.1029/GL007i006p00433.

Ball, S. M., D. R. Hanson and F. L. Eisele (1999). Laboratory studies of particle nucleation: Initial results for H2SO4, H2O, and NH3 vapors. J. of Geophys. Res., 104, D19, 23709-23718, doi: 10.1029/1999JD900411.

Baron P. A. and K. Willeke (2001). Aerosol measurement – Principles, Techniques and Applications, (2nd edition). John Wiley and Sons, New York.

Becker, R. and W. Döring (1935). Kinetische Behandlung der Keimbildung in übersättigten Dämpfen. Ann. Phys. 416, 8, 1521-3889, doi: 10.1002/andp.19354160806.

Benson, D., L.-H. Young, F. Kameel and S. H. Lee (2008). Laboratory-measured nucleation rates of sulfuric acid and water binary homogeneous nucleation from the SO2 + OH reaction. Geophys. Res. Lett., 35,11, L11801, doi:10.1029/2008GL033387.

Benson, D. R., M. E. Erupe and S. H. Lee (2009). Laboratory-measured H2SO4-H2O-NH3 ternary homogeneous nucleation rates: Initial observations. Geophys. Res. Letters, 36, L15818, doi: 10.1029/2009GL038728.

Benson, D. R., J. H. Yu, A. Markovich and S. H. Lee (2011). Ternary homogeneous nucleation of H2SO4, NH3, and H2O under conditions relevant to the lower troposphere. Atmos. Chem. Phys., 11, 4755-4766, doi: 10.5194/acp-11-4755-2011.

Berndt, T., F. Stratmann, S. Bräsel, J. Heintzenberg, A. Laaksonen and M. Kulmala (2008). SO2 oxidation products other than H2SO4 as a trigger of new particle formation. Part 1: Laboratory investigations. Atmos. Chem. Phys., 8, 6365-6374, doi: 10.5194/acp-8-6365-2008.

Berndt, T., F. Stratmann, M. Sipilä, J. Vanhanen, T. Petäjä, J. Mikkilä, A. Grüner, G. Spindler, L. R. Mauldin III, J. Curtius, M. Kulmala and J. Heintzenberg (2010). Laboratory study on new particle formation from the reaction OH + SO2: influence of experimental conditions, H2O vapour, NH3 and the amine tert-butylamine on the overall process. Atmos. Chem. Phys., 10, 7101-7116, doi: 10.5194/acp-10-7101-2010.

Berresheim, H., T. Elste, C. Plass-Dülmer, F. L. Eisele and D. J. Tanner (2000). Chemical ionization mass spectrometer for long-term measurements of atmospheric OH and H2SO4. Int. J. of Mass Spectr. 202, 1-3, 91-109, doi: 10.1016/S1387-3806(00)00233-5.

Brus, D., V. Ždímal and F. Stratmann (2006). Homogeneous nucleation rate measurements of 1-propanol in helium: The effect of carrier gas pressure. J. Chem. Phys. 124, 164306, doi: 10.1063/1.2185634.

Brus, D., A.-P. Hyvärinen, J. Wedekind, Y. Viisanen, M. Kulmala, V. Ždímal, J. Smolík and H. Lihavainen (2008). The homogeneous nucleation of 1-pentanol in a laminar flow diffusion chamber: The effect of pressure and kind of carrier gas. J. Chem. Phys. 128, 134312, doi: 10.1063/1.2901049.

Brus, D., A.-P. Hyvärinen, Y. Viisanen, M. Kulmala and H. Lihavainen (2010). Homogeneous nucleation of sulfuric acid and water mixture: experimental setup and first results. Atmos. Chem. Phys., 10, 2631-2641, doi: 10.5194/acp-10-2631-2010.

Dal Maso, M., M. Kulmala, I. Riipinen, R. Wagner, T. Hussein, P. P. Aalto and K. E. J. Lehtinen (2005). Formation and growth of fresh atmospheric aerosols: Eight years of aerosol size distribution from SMEAR II, Hyytiälä, Finland. Boreal Environ. Res., 10, 323–33.

Dal Maso, M., L. Sogacheva, P. P. Aalto, I. Riipinen, M. Komppula, P. Tunved, L. Korhonen, V. Suur-Uski, A. Hirsikko, T. Kurten, V.-M. Kerminen, H. Lihavainen, Y. Viisanen, H.-C. Hansson and M. Kulmala (2007). Tellus B, 59B, 350-361, doi: 10.1111/j.1600-0889.2007.00267.x.

Eisele, F. and D. Tanner (1993). Measurement of the gas phase concentration of H2SO4 and methanesulfonic acid and estimates of H2SO4 production and loss in the atmosphere. J. Geophys. Res., 98, D5, 9001-9010, doi: 10.1029/93JD00031.

Erupe, M. E., A. A. Viggiano and S.-H. Lee (2010). The effect of trimethylamine on atmospheric nucleation involving H_2SO_4. Atmos. Chem. Phys., 11, 4767-4775, doi: 10.5194/acp-11-4767-2011.

Ford, I. J. (2004). Statistical mechanics of nucleation: A review. J. Mech. Eng. Sci. 218, 883–899, doi: 10.1243/0954406041474183.

García, M., S. Rodríguez, Y. González and R. García (2014). Climatology of new particle formation at Izaña mountain GAW observatory in the subtropical North Atlantic. Atmos. Chem. Phys., 14, 3865–3881, doi: 10.5194/acp-14-3865-2014.

Graßmann, A. and F. Peters (2002). Homogeneous nucleation rates of n-propanol in nitrogen measured in a piston-expansion tube. J. Chem. Phys. 116, 7617, doi: 10.1063/1.1465400.

Guo, S., M. Hu, M. Zamora, J. Peng, D. Shang, J. Zheng, Z. Du, Z. Wu, M. Shao, L. Zeng, M. Molina, and R. Zhang (2014). Elucidating severe urban haze formation in China, PNAS, 111, 49, 17373-17378, doi: 10.1073/pnas.1419604111.

Hamed, A., J. Joutsensaari, S. Mikkonen, L. Sogacheva, M. Dal Maso, M. Kulmala, F. Cavalli, S. Fuzzi, M. C. Facchini, S. Decesari, M. Mircea, K. E. J. Lehtinen and A. Laaksonen (2007). Nucleation and growth of new particles in Po Valley, Italy. Atmos. Chem. Phys., 7, 355-376, doi: 10.5194/acp-7-355-2007.

Hering, S. and M. Stolzenburg (2005). A Method for Particle Size Amplification by Water Condensation in a Laminar, Thermally Diffusive Flow. Aerosol Sci. Tech., 39, 5, 428-436, doi: 10.1080/027868290953416.

Herrmann, E., D. Brus, A.-P. Hyvärinen, F. Stratmann, M. Wilck, H. Lihavainen and M. Kulmala (2010). A computational fluid dynamics approach to nucleation in the water-sulfuric acid–system. J. Phys. Chem. A, 114(31), 8033–8042, doi: 10.1021/jp103499q.

Hirsikko, A., L. Laakso, U. Hõrrak, P. P. Aalto, V.-M. Kerminen and M. Kulmala (2005). Annual and size dependent variation of growth rates and ion concentrations in boreal forest. Bor. Env. Res., 10, 357-369.

Hirsikko, A., T. Nieminen, S. Gagné, K. Lehtipalo, H. E. Manninen, M. Ehn, U. Hõrrak, V.-M. Kerminen, L. Laakso, P. H. McMurry, A. Mirme, S. Mirme, T. Petäjä, H. Tammet, V. Vakkari, M. Vana and M. Kulmala (2011). Atmospheric ions and nucleation: a review of observations, Atmos. Chem. Phys., 11, 767-798, doi: 10.5194/acp-11-767-2011.

Hyvärinen, A.-P., D. Brus, V. Ždímal, J. Smolík, M. Kulmala, Y. Viisanen and H. Lihavainen (2006). The carrier gas pressure effect in a laminar flow diffusion chamber, homogeneous nucleation of n-butanol in helium. J. Chem. Phys. 124, 224304. doi: 10.1063/1.2200341.

Hyvärinen, A.-P., D. Brus, V. Ždímal, J. Smolík, M. Kulmala, Y. Viisanen and H. Lihavainen (2008). Erratum: "The carrier gas pressure effect in a laminar flow diffusion chamber, homogeneous nucleation of n-butanol in helium" [J. Chem. Phys.124, 224304 (2006)]. J. Chem. Phys. 128, 109901, doi: 10.1063/1.2840353.

Hyvärinen, A.-P., D. Brus, J. Wedekind and H. Lihavainen (2010). How ambient pressure influences water droplet nucleation at tropospheric conditions. Geophys. Res. Lett., 37, 21, doi: 10.1029/2010GL045013.

Iida, K., M. R. Stolzenburg, P. H. McMurry and J. N. Smith (2008). Estimating nanoparticle growth rates from size-dependent charged fractions: Analysis of new particle formation events in Mexico City. J. Geophys. Res., 113, D05207, doi: 10.1029/2007JD009260.

Iida, K., M. R. Stolzenburg and P. R. McMurry (2009). Effect of working fluid on Sub-2 nm particle detection with a laminar flow ultrafine condensation particle counter, Aerosol Sci. Tech., 43, 1, 81-96, doi: 10.1080/02786820802488194.

Iland, K., J. Wölk, R. Strey and D. Kashchiev (2007). Argon nucleation in a cryogenic nucleation pulse chamber. J. Chem. Phys. 127, 154506, doi: 10.1063/1.2764486.

IPCC, 2013: Climate Change 2013: The Physical Science Basis. Contribution of Working Group I to the Fifth Assessment Report of the Intergovernmental Panel on Climate Change [Stocker, T.F., D. Qin, G.-K. Plattner, M. Tignor, S.K. Allen, J. Boschung, A. Nauels, Y. Xia, V. Bex and P.M. Midgley (eds.)]. Cambridge University Press, Cambridge, United Kingdom and New York, NY, USA, 1535 pp.

Jokinen, V. and J. M. Mäkelä (1997). Closed-loop arrangement with critical orifice for DMA sheath/ excess flow system. J. Aerosol Sci., 28, 4, 643-648, doi: 10.1016/S0021-8502(96)00457-0.

Jokinen, T., M. Sipilä, H. Junninen, M. Ehn, G. Lönn, J. Hakala, T. Petäjä, R. L. Mauldin III, M. Kulmala and D. R. Worsnop (2012). Atmospheric sulphuric acid and neutral cluster measurements using CI-APi-TOF. Atmos. Chem. Phys., 12, 4117-4125, doi: 10.5194/acp-12-4117-2012.

Junninen, H., M. Ehn, T. Petäjä, L. Luosujärvi, T. Kotiaho, R. Kostiainen, U. Rohner, M. Gonin, K. Fuhrer, M. Kulmala and D. R. Worsnop (2010). A high-resolution mass spectrometer to measure atmospheric ion composition. Atmos. Meas. Tech., 3, 1039–1053, doi: 10.5194/amt-3-1039-2010.

Junninen, H. (2014). Data cycle in atmospheric physics: from detected millivolts to understanding the atmosphere (Doctoral dissertation). Report Series in Aerosol Science, Helsinki 145. Retrieved from https://helda.helsinki.fi/handle/10138/42512

Järvinen, E., A. Virkkula, T. Nieminen, P. P. Aalto, E. Asmi, C. Lanconelli, M. Busetto, A. Lupi, R. Schioppo, V. Vitale, M. Mazzola, T. Petäjä, V.-M. Kerminen, and M. Kulmala (2013). Seasonal cycle and modal structure of particle number size distribution at Dome C, Antarctica. Atmos. Chem. Phys., 13, 7473–7487, doi: 10.5194/acp-13-7473-2013.

Kalikmanov, V. I. (2006). Mean-field kinetic nucleation theory. J. Chem. Phys. 124, 124505, doi: 10.1063/1.2178812.

Kashchiev, D. (1986). On the relation between nucleation work, nucleus size, and nucleation rate. J. Chem. Phys. 76, 5098, doi: 10.1063/1.442808.

Kerminen, V.-M., L. Pirjola and M. Kulmala (2001). How significantly does coagulational scavenging limit atmospheric particle production? J. Geophys. Res., 106(D20), 24119–24125, doi: 10.1029/2001JD000322.

Kerminen, V.-M., T. Petäjä, H. E. Manninen, P. Paasonen, T. Nieminen, M. Sipilä, H. Junninen, M. Ehn, S. Gagné, L. Laakso, I. Riipinen, H. Vehkamäki, T. Kurten, I. K. Ortega, M. Dal Maso, D. Brus, A.-P. Hyvärinen, H. Lihavainen, J. Leppä, K. E. J. Lehtinen, A. Mirme, S. Mirme, U. Horrãk, T. Berndt, F. Stratmann, W. Birmili, A. Wiedensohler A. Metzger, J. Dommen, U. Baltensperger, A. Kiendler-Scharr, T. F. Mentel, J. Wildt, P. M. Winkler, P. E. Wagner, A. Petzold, A. Minikin, C. Plass-Dülmer, U. Pöschl, A. Laaksonen and M. Kulmala (2010). Atmospheric nucleation: highlights of the EUCAARI project and future directions. Atmos. Chem. Phys., 10, 10829-10848, doi: 10.5194/acp-10-10829-2010.

Kirkby, J., J. Curtius, J. Almeida, E. Dunne, J. Duplissy, S. Ehrhart, A. Franchin, S. Gagné, L. Ickes, A. Kürten, A. Kupc, A. Metzger, F. Riccobono, L. Rondo, S. Schobesberger, G. Tsagkogeorgas, D. Wimmer, A. Amorim, F. Bianchi, M. Breitenlechner, A. David, J. Dommen, A. Downard, M. Ehn, R. Flagan, S. Haider, A. Hansel, D. Hauser, W. Jud, H. Junninen, F. Kreissl, A. Kvashin, A. Laaksonen, K. Lehtipalo, J. Lima, E. Lovejoy, V. Makhmutov, S. Mathot, J. Mikkilä, P. Minginette, S. Mogo, T. Nieminen, A. Onnela, P. Pereira, T. Petäjä, R. Schnitzhofer, J. Seinfeld, M. Sipilä, Y. Stozhkov, F. Stratmann, A. Tomé, J. Vanhanen, Y. Viisanen, A. Vrtala, P. Wagner, H. Walther, E. Weingartner, H. Wex, P. Winkler, K. Carslaw, D. Worsnop, U. Baltensperger and M. Kulmala (2011). Role of sulphuric acid, ammonia and galactic cosmic rays in atmospheric aerosol nucleation. Nature, 476, 429-433, doi:10.1038/nature10343.

Komppula M., M. Dal Maso, H. Lihavainen, P. P. Aalto, M. Kulmala and Y. Viisanen. Comparison of new particle formation events at two locations in northern Finland. Bor. Env. Res., 8, 395-404.

Korhonen, P., M. Kulmala, A. Laaksonen, Y. Viisanen, R. McGraw and J. H. Seinfeld (1999). Ternary nucleation of H2SO4, NH3 and H2O in the atmosphere. J. Geophys. Res., 104, 26349-26353, doi: 10.1029/1999JD900784.

Kousaka, Y., T. Niida, K. Okyama and H. Tanaka (1982). Development of a mixing type condensation nucleus counter. J Aerosol Sci., 13, 3, 231-240, doi: 10.1016/0021-8502(82)90064-7.

Kuang, C., P. H. McMurry, A. V. McCormick and F. L. Eisele (2008). Dependence of nucleation rates on sulfuric acid vapor concentration in diverse atmospheric locations. J. Geophys. Res., 113, D10, doi: 10.1029/2007JD009253.

Kuang C., M. Chen, J. Zhao, J. Smith, P. H. McMurry and J. Wang (2012). Size and time-resolved growth rate measurements of 1 to 5 nm freshly formed atmospheric nuclei. Atmos. Chem. Phys., 12, 3573–3589, doi: 10.5194/acp-12-3573-2012.

Kulmala, M. (1988). Nucleation as an aerosol physical problem (Doctoral dissertation). Report Series in Aerosol Science, 0356-0961 ; 52. Department of Physics, University of Helsinki, Finland. Retrieved from: https://www.kansalliskirjasto.finna.fi/Record/helka.61865

Kulmala, M. and A. Laaksonen (1990). Binary nucleation of water–sulfuric acid system: Comparison of classical theories with different H2SO4 saturation vapor pressures. J. Chem. Phys., 93, 1, 696, doi: 10.1063/1.459519.

Kulmala, M., M. Dal Maso, J. M. Mäkelä, L. Pirjola, M. Väkevä, P. P. Aalto, P. Miikkulainen, K. Hämeri and C. O'Dowd (2001). On the formation, growth and composition of nucleation mode particles. Tells B, 53, 4, 479-490, doi: 10.1034/j.1600-0889.2001.530411.x.

Kulmala M. (2003). How particles nucleate and grow. Science, 302, 5647, 1000-1001, doi: 10.1126/science.1090848.

Kulmala M., H. Vehkamäki, T. Petäjä, M. Dal Maso, A. Lauri, V.-M. Kerminen, W. Birmili and P. H. McMurry (2004b). Formation and growth rates of ultrafine atmospheric particles: a review of observations. J. Aerosol. Sci., 35, 143-176, doi:10.1016/j.jaerosci.2003.10.003.

Kulmala M., K. E. J. Lehtinen and A. Laaksonen (2006). Cluster activation theory as an explanation of the linear dependence between formation rate of 3nm particles and sulphuric acid concentration. Atmos. Chem. Phys., 6, 787-793, doi: 10.5194/acp-6-787-2006.

Kulmala, M., I. Riipinen, M. Sipilä, H. E. Manninen, T. Petäjä, H. Junninen, M. Dal Maso, G. Mordas, A. Mirme, M. Vana, A. Hirsikko, L. Laakso, R. M. Harrison, I. Hanson, C. Leung, K. E. J. Lehtinen and V.-M. Kerminen (2007). Towards direct measurement of atmospheric nucleation. Science, 318, 89, doi: 10.1126/science.1144124.

Kurtén, T., T. Petäjä, J. Smith, I. K. Ortega, M. Sipilä, H. Junninen, M. Ehn, H. Vehkamäki, L. Mauldin III, D. R. Worsnop and M. Kulmala (2011). The effect of H2SO4 – amine clustering on chemical ionization mass spectrometry (CIMS) measurements of gas-phase sulfuric acid. Atmos. Chem. Phys., 11, 3007-3019, doi: 10.5194/acp-11-3007-2011.

Kürten, A., J. Curtius, B. Nillius and S. Borrmann (2005). Characterization of an Automated, Water-Based Expansion Condensation Nucleus Counter for Ultrafine Particles. Aerosol Sci. Tech., 39, 12, 1174-1183, doi: 10.1080/02786820500431355.

Kürten, A., L. Rondo, S. Ehrhart and J. Curtius (2012). Calibration of a Chemical Ionization Mass Spectrometer for the Measurement of Gaseous Sulfuric Acid. J. Phys. Chem. A, 116, 6375-6386, doi: 10.1021/jp212123n.

Laakso, L. T. Petäjä, K. E. J. Lehtinen, M. Kulmala, J. Paatero, U. Hõrrak, H. Tammet and J. Joutsensaari (2004). Ion production rate in a boreal forest based on ion, particle and radiation measurements. Atmos. Chem. Phys., 4, 1933-1943, doi: 10.5194/acp-4-1933-2004.

Lee, S.-H., J. M. Reeves, J. C. Wilson, D. E. Hunton, A. A. Viggiano, T. M. Miller, J. O. Ballenthin and L. R. Lait (2003). Particle Formation by Ion Nucleation in the Upper Troposphere and Lower Stratosphere. Science, 301, 5641, 1886-1889, doi: 10.1126/science.1087236.

Lihavainen, H. (2000). Laminar Flow Diffusion Chamber for Homogeneous Nucleation Studies (Doctoral dissertation). Report series: Aerosol Science, Helsinki University, Finland.

Lihavainen, H. and Y. Viisanen (2001). A Laminar Flow Diffusion Chamber for Homogeneous Nucleation Studies. J. Phys. Chem. B, 105 (47), 11619–11629, doi: 10.1021/jp011189j.

Lihavainen, H., V.-M. Kerminen, M. Komppula, J. Hatakka, V. Aaltonen, M. Kulmala, and Y. Viisanen (2003). Production of "potential" cloud condensation nuclei associated with atmospheric new-particle formation in northern Finland. J. Geophys. Res., 108(D24), 4782, doi: 10.1029/2003JD003887.

Lohmann, U. and J. Feichter (2005). Global indirect aerosol effects: a review. Atmos. Chem. Phys., 5, 715–737, doi:10.5194/acp-5-715-2005.

Lovejoy, E. R., J. Curtius and K. D. Froyd (2004). Atmospheric ion-induced nucleation of sulphuric acid and water. J. Geophys. Res., 109, D08204, doi: 10.1029/2003JD004460.

Manka, A. A., D. Brus, A.-P. Hyvärinen, H. Lihavainen, J. Wölk and R. Strey (2010). Homogeneous water nucleation in a laminar flow diffusion chamber. J. Chem. Phys. 132, 244505, doi: 10.1063/1.3427537.

Manninen, H. E., T. Nieminen, E. Asmi, S. Gagné, S. Häkkinen, K. Lehtipalo, P. Aalto, M. Vana, A. Mirme, S. Mirme, U. Hõrrak, C. Plass-Dülmer, G. Stange, G. Kiss, A. Hoffer, N. Törö, M. Moerman, B. Henzing, G. de Leeuw, M. Brinkenberg, G. N. Kouvarakis, A. Bougiatioti, N. Mihalopoulos, C. O'Dowd, D. Ceburnis, A Arneth, B. Svenningsson, E. Swietlicki, L. Tarozzi, S. Decesari, M. C. Facchini, W. Birmili, A. Sonntag, A. Wiedensohler, J. Boulon, K. Sellegri, P. Laj, M. Gysel N. Bukowiecki, W. Weingartner, G. Wehrle, A. Laaksonen, A. Hamed, J. Joutsensaari, T. Petäjä, V.-M. Kerminen and M. Kulmala (2010). EUCAARI ion spectrometer measurements at 12 European sites - analysis of new particle formation events. Atmos. Chem. Phys., 10, 7907-7927, doi: 10.5194/acp-10-7907-2010.

Mauldin III, R. L., G. Frost, G. Chen, D. Tanner, A. Prevot, D. Davis and F. Eisele (1998). OH measurements during the First Aerosol Characterization Experiment (ACE 1): Observations and model comparisons. J. Geophys. Res., 103, 16713-16729, doi:10.1029/98JD00882.

Menon, S., J. Hansen, L. Nazarenko and Y. Luo (2002). Climate effects of black carbon aerosols in China and India. Science 297, 2250, doi: 10.1126/science.1075159.

McMurry, P. H (1980). Photochemical aerosol formation from SO2: A theoretical analysis of smog chamber data. J. Colloid. Interf. Sci., 78, 2, 513-527, doi: 10.1016/0021-9797(80)90589-5.

McMurry, P. H (2000). The History of Condensation Nucleus Counters. Aerosol Sci. Tech., 33, 4, 297-322, doi: 10.1080/02786820050121512.

Merikanto, J., D. V. Spracklen, G. W. Mann, S. J. Pickering, and K. S. Carslaw (2009). Impact of nucleation on global CCN. Atmos. Chem. Phys., 9, 8601-8616, doi: 10.5194/acp-9-8601-2009.

Metzger, A., B. Verheggen, J. Dommen, J. Duplissy, A. S. H. Prevot, E. Weingartner, I. Riipinen, M. Kulmala, D. V. Spracklen, K. S. Carslaw and U. Baltensperger (2010). Evidence for the role of organics in aerosol particle formation under atmospheric conditions. PNAS, 107, 15, 6646-6651, doi: 10.1073/pnas.0911330107.

Mäkelä, J. M., M. Dal Maso, L. Pirjola, P. Keronen, L. Laakso, M. Kulmala and A. Laaksonen (2000). Characteristics of the atmospheric particle formation events observed at a boreal forest site in Southern Finland. Boreal Env. Res., 5, 299-313.

Mönkkönen, P., I. K. Koponen, K. E. J. Lehtinen, K. Hämeri, R. Uma and M. Kulmala (2005). Measurements in a highly polluted Asian mega city: observations of aerosol number size distribution, modal parameters and nucleation events. Atmos. Chem. Phys., 5, 57–66, doi: 10.5194/acp-5-57-2005.

Napari, I., M. Noppel, H. Vehkamäki and M. Kulmala (2002). Parametrization of ternary nucleation rates for H2SO4-NH3-H2O vapors. J. Geophys. Res., 107(D19), 4381, doi: 10.1029/2002JD002132.

Napari, I. and A. Laaksonen (2007). Surface tension and scaling of critical nuclei in diatomic and triatomic fluids. J. Chem. Phys. 126, 134503, doi: 10.1063/1.2714950.

Nieminen, T., P. Paasonen, H. E. Manninen, K. Sellegri, V.-M. Kerminen and M. Kulmala (2011). Parameterization of ion-induced nucleation rates based on ambient observations. Atmos. Chem. Phys., 11, 3393-3402, doi: 10.5194/acp-11-3393-2011.

Nishita, C., K. Osada, M. Kido, K. Matsunaga and Y. Iwasaka (2008). Nucleation mode particles in upslope valley winds at Mount Norikura, Japan: Implications for the vertical extent of new particle formation events in the lower troposphere. J. Geophys. Res., 113(D6), doi: 10.1029/2007JD009302.

O'Dowd, C., P. Aalto, K. Hämeri, M. Kulmala and T. Hoffmann (2002a). Aerosol formation: Atmospheric particles from organic vapors. Nature, 416, 497-498, doi: 10.1038/416497a.

Oxtoby, D. W. and R. Evans (1988). Nonclassical nucleation theory for the gas–liquid transition. J. Chem. Phys. 89, 7521, doi: 10.1063/1.455285

Paasonen, P., T. Nieminen, E. Asmi, H. E. Manninen, T. Petäjä, C. Plass-Dülmer, H. Flentje, W. Birmili, A. Wiedensohler, U. Horrãk, A. Metzger, A. Hamed, A. Laaksonen, M. C. Facchini, V.-M. Kerminen and M. Kulmala (2010). On the roles of sulphuric acid and low-volatility organic vapors in the initial steps of atmospheric new particle formation. Atmos. Chem. Phys., 10, 11223-11242, doi: 10.5194/acp-10-11223-2010.

Petäjä, T., L. R. Mauldin III, E. Kosciuch, J. McGrath, T. Nieminen, P. Paasonen, M. Boy, A. Adamov, T. Kotiaho and M. Kulmala (2009). Sulfuric acid and OH concentrations in a boreal forest site. Atmos. Chem. Phys., 9, 7435-7448, doi: 10.5194/acp-9-7435-2009.

Raatikainen, T., A.-P. Hyvärinen, J. Hatakka, T. S. Panwar, R. K. Hooda, V. P. Sharma and H. Lihavainen (2011). Comparison of aerosol properties from the Indian Himalayas and the Indo-Gangetic plains. Atmos. Chem. Phys. Discuss., 11, 11417-11453, doi: 10.5194/acpd-11-11417-2011.

Richardson, C. B., R. L. Hightower and A. L. Pigg (1986). Optical measurements of evaporation of sulphuric acid droplets. Applied Optics, 25, 7, 1226-1229, doi: 10.1364/AO.25.001226.

Riipinen, I., S.-L. Sihto, M. Kulmala, F. Arnold, M. Dal Maso, W. Birmili, K. Saarnio, K. Teinilä, V.-M. Kerminen, A. Laaksonen and K. E. J. Lehtinen (2007). Connections between atmospheric sulphuric acid and new particle formation during QUEST III–IV campaigns in Heidelberg and Hyytiälä. Atmos. Chem. Phys., 7, 1899-1914, doi: 10.5194/acp-7-1899-2007.

Seok, C. and D. W. Oxtoby (1998). Nucleation in n-alkanes: A density-functional approach. J. Chem. Phys. 109, 7982, doi: 10.1063/1.477445.

Seinfeld, J. H. and S. N. Pandis (1998). Atmospheric chemistry and physics: From air pollution to climate change. John Wiley & Sons Inc., New York.

Sgro, L. A. and J. de la Mora (2004). Aerosol Sci. Technol., 38, 1, 1-11, doi: 10.1080/02786820490247560.

Shaw, G.E. (1988). Antarctic aerosols: A review. Reviews of Geophysics, 26, 89-112.

Sihto, S.-L. M. Kulmala, V.-M. Kerminen, M. Dal Maso, T. Petäjä, I. Riipinen, H. Korhonen, F. Arnold, R. Janson, M. Boy, A. Laaksonen and K. E. J. Lehtinen (2006). Atmospheric sulphuric acid and aerosol formation: implications from atmospheric measurements for nucleation and early growth mechanisms. Atmos. Chem. Phys., 6, 4079-4091, doi: 10.5194/acp-6-4079-2006.

Sipilä, M., T. Berndt, T. Petäjä, D. Brus, J. Vanhanen, F. Stratmann, J. Patokoski, R. L. Mauldin III, A.-P. Hyvärinen, H. Lihavainen and M. Kulmala (2010). The role of sulphuric acid in atmospheric nucleation. Science, 327, 5970, 1243-1246, doi: 10.1126/science.1180315.

Škrabalová L., D. Brus, T. Anttila, V. Ždímal and H. Lihavainen (2014). Growth of sulphuric acid nanoparticles under wet and dry conditions. Atmos. Chem. Phys. 14, 6461-6475, doi: 10.5194/acp-14-6461-2014.

Slanina, J., H. M. ten Brink, R. P. Otjes, A. Even, P. Jongejan, S. Khlystov, A. Waijers-Ijpelaan, M. Hu and Y.Lu (2001). The continuous analysis of nitrate and ammonium in aerosols by the steam jet aerosol collector (SJAC): extension and validation of the methodology. Atmos. Environ., 35, 2319-2330, doi: 10.1016/S1352-2310(00)00556-2.

Smith, J. N., K. F. Moore, F. L. Eisele, D. Voisin, A. K. Ghimire, H. Sakurai and P. H. McMurry (2005). Chemical composition of atmospheric nanoparticles during nucleation events in Atlanta. J. Geophys. Res., 110, D22S03, doi: 10.1029/2005JD005912.

Stockwell, W. R. and J. G. Calvert (1983) The mechanism of the OH-SO_2 reaction. Atmos. Env., 17, 11, 2231-2235, doi: 10.1016/0004-6981(83)90220-2.

Stohl, A., G. Wotawa, P. Seibert and H. Kromp-Kolb (1995). Interpolation errors in wind fields as a function of spatial and temporal resolution and their impact on different types of kinematic trajectories. J. Appl. Meteor., 34, 2149–2165, doi: 10.1175/1520-0450(1995)034<2149:ieiwfa>2.0.co;2.

Stolzenburg, M. R. (1988). An ultrafine aerosol size distribution measuring system. PhD thesis, Mechanical engineering department, University of Minnesota, Minneapolis.

Strey, R. T. Schmeling and P.E. Wagner (1986a). Experimental nucleation rates of the n-alcohols in comparison with theory. J. Aerosol Sci., 17, 3, 462.

Strey, R. T. Schmeling and P.E. Wagner (1986b). Homogeneous nucleation rates for n-alcohol vapors measured in a two-piston expansion chamber. J. Chem. Phys. 84, 2325, doi: 10.1063/1.450396.

ten Brink, H., R. Otjes, P. Jongejan and S. Slanina (2007). An instrument for semi-continuous monitoring of the size-distribution of nitrate, ammonium, sulphate and chloride in aerosol. Atmos. Environ., 41, 13, 2768-2779, doi: 10.1016/j.atmosenv.2006.11.041.

Twomey, A. (1974). Pollution and the planetary albedo. Atmos. Env., 8, 1251-1256.

Twomey, S. (1991). Aerosols, clouds and radiation. Atmos. Env., 25A, 2435-2442.

Vanhanen, J., J. Mikkilä, K. Lehtipalo, M. Sipilä, H. E. Manninen, E. Siivola, T. Petäjä and M. Kulmala (2011). Particle Size Magnifier for Nano-CN Detection. Aerosol Sci. Tech., 45, 4, 533-542, doi: 10.1080/02786826.2010.547889.

Vehkamäki, H., M. Kulmala, I. Napari, K. E. J. Lehtinen, C. Timmreck, M. Noppel and A. Laaksonen (2002). An improved parameterization for sulfuric acid-water nucleation rates for tropospheric and stratospheric conditions. J. Geophys. Res., 107(D22), 4622, doi: 10.1029/2002JD002184.

Venzac, H., K. Sellegri, P. Laj, P. Villani, P. Bonasoni, A. Marinoni, P. Cristofanelli, F. Calzolari, S. Fuzzi, S. Decesari, M.-C. Facchini, E. Vuillermoz and G. P. Verza (2008). High Frequency New Particle Formation in the Himalayas. PNAS, 105(41), 15666–15671, doi: 10.1073/pnas.0801355105.

Viisanen, Y., M. Kulmala and A. Laaksonen (1997). Experiments on gas-liquid nucleation of sulfuric acid and water. J. Chem. Phys. 107, 3, 920-926, doi: 10.1063/1.474445.

Weber, R. J., J. J. Marti, P. H. McMurry, F. L. Eisele, D. J. Tanner and A. Jefferson (1996). Measured atmospheric new particle formation rates: Implications for nucleation mechanisms. Chem. Eng. Commun., 151, 1, 53-64, doi: 10.1080/00986449608936541.

Weber, R. J., J. J. Marti, P. H. McMurry, F. L. Eisele, D. J. Tanner and A. Jefferson (1997). Measurements of new particle formation and ultrafine particle growth rates at a clean continental site. J. Geophys. Res., 102, D4, 4375-4385, doi: 10.1029/96JD03656.

Wedekind, J., A.-P. Hyvärinen, D. Brus, and D. Reguera (2008). Unraveling the "Pressure Effect" in Nucleation. Phys. Rev. Lett. 101, 125703, doi: 10.1103/PhysRevLett.101.125703.

Weller, R., A. Minikin, D. Wagenbach and V. Dreiling (2011). Characterization of the interannual, seasonal, and diurnal variations of condensation particle concentrations at Neumayer, Antarctica. Atmos. Chem. Phys., 11, 13243–13257, doi: 10.5194/acp-11-13243-2011.

Wiedensohler, A. and H. J. Fissan (1991). Bipolar Charge Distributions of Aerosol Particles in High-Purity Argon and Nitrogen. Aerosol Sci. and Tech., 14, 3, 358-364, doi: 10.1080/02786829108959498.

Wilson, C. (1897). Condensation of Water Vapour in the Presence of Dust-free Air and other Gases. Transactions of the Royal Society. London, A189, 265-307.

Winkler, P. M., G. Steiner, A. Vrtala, H. Vehkamäki, M. Noppel, K. E. J. Lehtinen, G. P. Reischl, P. E. Wagner and M. Kulmala (2008a). Heterogeneous Nucleation Experiments Bridging the Scale from Molecular Ion Clusters to Nanoparticles. Science, 319, 5868, 1374-1377, doi: 10.1126/science.1149034.

Winkler, P. M., A. Vrtala and P. E. Wagner (2008b). Condensation particle counting below 2 nm seed particle diameter and the transition from heterogeneous to homogeneous nucleation. Atmos. Res., 90, 125-131, doi: 10.1016/j.atmosres.2008.01.001.

Winklmayr, W., G.P. Reischl, A.O. Lindner and A. Berner (1991). A new electromobility spectrometer for the measurement of aerosol size distributions in the size range from 1 to 1000 nm. J. of Aer. Sci., 22, 3, 289-296, doi: 10.1016/S0021-8502(05)80007-2.

Wyslouzil, B. E., J. H. Seinfeld and R. C. Flagan (1991). Binary nucleation in acid-water systems. I. Methanesulfonic acid-water. J. Chem. Phys. 94, 6842, doi: 10.1063/1.460261.

Wyslouzil, B. E. and J. H. Seinfeld (1992). Nonisothermal homogeneous nucleation. J. Chem. Phys. 97, 2661, doi: 10.1063/1.463055.

Wu, Z., M. Hu, S. Liu, B. Wehner, S. Bauer, A. Ma ßling, A. Wiedensohler, T. Petäjä, M. Dal Maso, and M. Kulmala (2007). New particle formation in Beijing, China: Statistical analysis of a 1-year data set. J. Geophys. Res., 112, D09209, doi: 10.1029/2006JD007406.

Wölk, J. and R. Strey (2001). Homogeneous Nucleation of H2O and D2O in Comparison: The Isotope Effect. J. Phys. Chem. B 105, 11683–11701, doi: 10.1021/jp0115805.

Xiao, S., M. Y. Wang, L. Yao, M. Kulmala, B. Zhou, X. Yang, J. M. Chen, D. F. Wang, Q. Y. Fu, D. R. Worsnop and L. Wang (2015). Strong atmospheric new particle formation in

winter in urban Shanghai, China. Atmos. Chem. Phys., 15, 1769–1781, doi: 10.5194/acp-15-1769-2015.

Young, L., D. Benson, F. Kameel, J. Pierce, H. Junninen, M. Kulmala and S. H. Lee (2008). Laboratory studies of H2SO4/H2O binary homogeneous nucleation from the SO2+OH reaction: evaluation of the experimental setup and preliminary results. Atmos. Chem. Phys., 8, 4997-5016, doi: 10.5194/acp-8-4997-2008.

Yu, F (2006). From molecular clusters to nanoparticles: second-generation ion-mediated nucleation model. Atmos. Chem. Phys., 6, 5193-5211, doi: 10.5194/acp-6-5193-2006.

Yu, F., Z. Wang, G. Luo and R. Turco (2008). Ion-mediated nucleation as an important global source of tropospheric aerosols. Atmos. Chem. Phys., 8, 2537-2554, doi: 10.5194/acp-8-2537-2008.

Yu, F (2010). Ion-mediated nucleation in the atmosphere: Key controlling parameters, implications, and look-up table. J. Geophys. Res., 115, D03206, doi: 10.1029/2009JD012630.

Zhang, R., I. Suh, J. Zhao, D. Zhang, E. C. Fortner, X. Tie, L. T. Molina, M. J. Molina (2004). Atmospheric New Particle Formation Enhanced by Organic Acids. Science, 304,5676, 1487-1490, doi: 10.1126/science.1095139.

Zhang, R. (2010). Getting to the Critical Nucleus of Aerosol Formation. Science, 328, 5984, 1366-1367, doi: 10.1126/science.1189732.

Zheng, J., A. Khalizov, L. Wang and R. Zhang (2010). Atmospheric Pressure-Ion Drift Chemical Ionization Mass Spectrometry for Detection of Trace Gas Species. Anal. Chem., 82, 7302-7308, doi: 10.1021/ac101253n.

Zollner, J. H., W. A. Glasoe, B. Panta, K. K. Carlson, P. H. McMurry and D. R. Hanson (2012). Sulfuric acid nucleation: power dependencies, variation with relative humidity, and effect of bases. Atmos. Chem. Phys., 12, 4399-4411, doi: 10.5194/acp-12-4399-2012.

REPORT SERIES IN AEROSOL SCIENCE

Editorial Board:
Prof. Kaarle Hämeri
Prof. Jorma Jokiniemi
Prof. Veli-Matti Kerminen
Prof. Markku Kulmala

Editor in Chief
Jenni Kontkanen

AEROSOLITUTKIMUSSEURA ry
(FINNISH ASSOCIATION FOR AEROSOL RESEARCH, FAAR)
c/o Antti Lauri, Department of Physics,
P. O. Box 64, FI-00014 University of Helsinki

http://www.atm.helsinki.fi/FAAR/
Email: faar-rs@helsinki.fi

Chairman: Antti Lauri
Vice Chairman: Miikka Dal Maso
Secretary: Jussi Malila
Treasurer: Niku Kivekäs

Board of FAAR (2015)
Jyrki Mäkelä (Kaarle Hämeri)
Helmi Keskinen (Mikael Ehn)
Mika Komppula (Anna Lähde)
Hilkka Timonen (Hannele Korhonen)

Aerosolitutkimusseura ry
Helsinki, 2015

Unigrafia 2015